NCCC-134
APPLIED COMMODITY PRICE ANALYSIS, FORECASTING AND MARKET RISK MANAGEMENT

On the Dependence Structure of European Vegetable Oil Markets

by

Romain Menier, Guillaume Bagnarosa,
and Alexandre Gohin

Suggested citation format:
Menier, R., G. Bagnarosa, and A. Gohin. 2022. "On the Dependence Structure of European Vegetable Oil Markets." Proceedings of the NCCC-134 Conference on Applied Commodity Price Analysis, Forecasting, and Market Risk Management. [http://www.farmdoc.illinois.edu/nccc134].

On the dependence structure of European vegetable oil markets

Romain Menier, Guillaume Bagnarosa, and Alexandre Gohin [1]

Paper presented at the NCCC-134 Conference on Applied Commodity Analysis, Forecasting, and Market Risk Management, 2022.

[1]Romain Menier is Quant and PhD Student in Saipol, Avril Group, Institut Agro, Rennes School of Business, and INRAe, UMR SMART (France).
Guillaume Bagnarosa is Associate Professor of Finance in Rennes School of Business.
Alexandre Gohin is Research Director in INRAe, UMR SMART.
Address all correspondence to Romain Menier by e-mail at `romain.menier@groupeavril.com`

On the dependence structure of European vegetable oil markets

March 27, 2022

Abstract

Motivated by the current context of high and volatile energy and food prices, we examine the conditional variance-covariance matrix dynamics and price discovery process characterising European vegetable oils. In addition to outcomes differences using daily or monthly datasets, we find that both the marginal distributions and volatility dependence structures relate to distinct economic fundamentals. The energy price mainly influences the vegetable oil trend component, and stock-to-use ratios are crucial for variance-covariance dynamics once their particular cold filter plugging point is considered. This latter point also reveals interesting interplays among vegetable oils according to the economic concepts of complementarity and substitutability.

JEL Classification— Q11, Q14, C32
Keywords— Vegetable oil, Price discovery, Volatility

1 Introduction

The current global context of inflationary pressures and soaring and highly volatile energy prices, which can partly be explained by the recent coronavirus pandemic and the Russian-Ukrainian conflict, has reawakened the debate on the food–energy nexus. Although this topic was extensively studied ten years ago (see Serra and Zilberman (2013) for a review of the literature), the current market environment is notably different from that prevailing earlier this century, and this justifies its reconsideration in this article. The reasons behind the emergence of these changes are threefold. First, biodiesel production, being the most direct transmission channel of energy price shocks towards food prices, greatly increased in the 2000s, and this was bolstered by successive government measures for reinforcing local energy-security policy and for mitigating global warming. In contrast, in the last few years, these public policies on biofuels and biofuel production have globally stabilised. Second, the financialisation of commodity markets originating in the early 2000s was at that time raising concerns about the price impact of speculators (Cheng & Xiong, 2014; Chkili et al., 2014). However, the accompanying significant increase of traded volumes on futures markets has recently been less pronounced, suggesting that other fundamental variables should be considered to justify the currently observed price pressures. Third, recent policy shifts such as trade wars (in particular between US and China), and more importantly a global pandemic, lead us to presume a change in vegetable oil market dynamics.

In this article, we thus focus on the European vegetable oil markets with the purpose of understanding their associated relative price levels and volatilities. These are very important input parameters for private stakeholders' investment decisions and hedging strategies, and they are also crucial for public decision-makers in assessing the impacts of their measures upon interlinked vegetable oil markets (Serra et al., 2011). This is even more relevant in developing

economies, where consumers spend over 80% of their income on food while producers strive to set up risk-management strategies (Prakash et al., 2011).

In addition to revisiting the previous literature against the current backdrop of increasing prices and volatility, this article makes three significant empirical and methodological contributions. First, we include in our analysis rapeseed oil, soybean oil, and palm oil, which are the three main feedstocks used for European biodiesel production (denoted hereafter RSO, PMO, and SBO, respectively). To do this, we resort to a unique vegetable oil daily price database and show how different the results are when using daily instead of monthly prices (an approach applied in previous literature). To the best of our knowledge, no study has purposely focused on the nexus of the different major vegetable oils and their links with the energy market in the EU.[1] Second, we also contribute to nonlinear price volatility transmission modelling, which is particularly relevant in commodities markets where price volatility asymmetries are very prevalent with stocks. We extend the analytical formula of the volatility impulse response function proposed by Hafner and Herwartz (2006) in the presence of price volatility asymmetry. Furthermore, we derive the necessary conditions to ensure covariance stationarity, while price volatility asymmetry and exogenous fundamental variables have been added to the spillover framework described by Fengler and Herwartz (2018), following Diebold and Yilmaz (2009, 2012). Third, this addition of a wide range of explanatory variables related to market fundamentals permits distinguishing between the phenomena of market contagion and market connectiveness. Indeed, in a multivariate setting, Bekaert et al. (2005) defined the volatility contagion between markets as being the excess correlation that is not explained by economic fundamentals. Serra and Zilberman (2013) likewise defined price volatility as 'a directionless price variability that cannot be predicted by market fundamentals'.

In our empirical study, we identify the fundamental variables related specifically to vegetable oils and biofuel production. Following Casassus et al. (2013), who developed the economic theory of storage to a multi-commodity setting, we rely on the economic concepts of substitutability and complementarity, which allow us to interpret the conditional variance–covariance dynamics of European vegetable oils taking into consideration their respective technical and industrial specificities. There is a rich economic literature, based on storage theory, telling us how the inventory levels of a storable commodity impact its associated price and volatility. However, there are few if any articles regarding inventory cross-impacts among commodities sharing a substitutability or complementarity relationship. In this article, we relate these economic concepts to technical industrial specificities, in particular the cold filter plugging point (CFPP), and to the global agricultural landscape.

The remainder of this paper is organised as follows. Section 2 will present the methodological aspects, Section 3 is devoted to description of the data and model selection, and Section 4 will analyse the empirical results. Finally, conclusions are given in Section 5.

[1] Serra and Zilberman (2013) reviewed 17 articles on price volatility transmission, and only two of them focused on the EU markets. Thereafter, Abdelradi and Serra (2015) studied the relationship between RSO and biodiesel in the EU markets and found that they share a common long-run equilibrium that stems from biodiesel production. Hasanov et al. (2016) complemented this finding by showing that crude oil instability propagates to both vegetable oil volatilities and prices. Nevertheless, in their study, they considered sunflower oil instead of PMO. Using the method of Diebold and Yilmaz (2012), Barbaglia et al. (2020) recently found that, even for non-biofuel crops, there is a bidirectional volatility spillover effect with energy prices. However, neither RSO nor PMO were included. Finally, Hasanov et al. (2018), who concluded that an asymmetric generalised autoregressive conditional heteroskedasticity (GARCH) model with structural breaks should be considered for agricultural markets, only studied univariate time series and considered soybeans instead of SBO.

2 Methodology

Several articles in the financial econometric literature have included fundamental covariates in the dynamics of both the conditional mean and variance. The interest in these models comes from their ability to complement the dynamics of the conditional moments based on their own past or lagged values with more complex dynamics associated with macroeconomic variables, which can be either stationary or non-stationary (Francq & Thieu, 2019; Han & Park, 2012).

2.1 Econometric model

For this study of European vegetable oils, we apply an approach using: the vector error correction model (VECM); the Baba, Engle, Kraft, and Kroner (BEKK) model; the Glosten, Jagannathan, and Runkle (GJR) model; and multivariate generalised autoregressive conditional heteroskedasticity (MGARCH). This is augmented by exogeneous variables in both the conditional mean and conditional variance (Silvennoinen & Teräsvirta, 2009). We term this the VECM–BEKK–GJR–MGARCH model, and it is described by

$$\begin{cases} \Delta P_t & = \alpha\beta^\tau P_{t-1} + \sum_{i=1}^{p} \Gamma_i \Delta P_{t-i} + C_t^V + \varepsilon_t \\ \Sigma_{t|t-1} & = C_t^G C_t^{G\tau} + A^\tau \varepsilon_{t-1}\varepsilon_{t-1}^\tau A + B^\tau \Sigma_{t-1|t-2} B + D^\tau \xi_{t-1}\xi_{t-1}^\tau D \end{cases} \quad \begin{cases} C_t^V & = \sum_{k=1}^{K_V} C_{z_k}^V z_{k,t} \\ C_t^G & = \sum_{k=0}^{K_G} C_{z_k}^G z_{k,t} \end{cases} \tag{1}$$

where: $\Sigma_{t|t-1}$ is the variance–covariance matrix of the complex at time t such that $\Sigma_{t|t-1} = E[\varepsilon_t\varepsilon_t^\tau|\mathcal{F}_{t-1}]$, with $\mathcal{F}_{t-1}$ being all the information available on the market at time $t-1$; α and β are $(K \times r)$ matrices with r being the cointegration rank; z_k represents the exogenous variables, with $z_{0,t} = 1$ for all t; $C_{z_k}^V$ represents $(K_V \times 1)$ matrices; and $C_{z_k}^G$ represents $(K_G \times K_G)$ matrices. We followed the representation given by Moschini and Myers (2001) to preserve the positive definiteness of the variance–covariance matrix and to avoid constraining the sign of the effects of the exogenous variables on price volatility. Furthermore, the last term in the conditional variance equation (equation (1)), $\xi_t = \varepsilon_t \circ \mathbb{1}_{x>0}(\varepsilon_t)$, in which $\circ$ denotes the Hadamard product, captures asymmetries in the price volatility dynamics. In stock markets, it is widely known that asymmetries take place with price decreases, but in commodity markets where storage is possible, asymmetries are associated with price increases (Ng & Pirrong, 1994; Zhen et al., 2018).

With regard to the model estimation, we can clearly see that vegetable oil prices are non-stationary and non-Gaussian time series, especially for daily data frequency[2] (see Table A1 of Appendix A). Assuming a Gaussian distribution thus leads to a consistent quasi-maximum-likelihood estimator (QMLE) whose limit distribution is Gaussian. It is worth mentioning that this property holds under particular conditions even though unit-root or near-unit-root covariates are added within the conditional moment dynamics (Han & Park, 2012). This will be the case when we consider the inventories in level or in difference as covariates. Furthermore, Hasanov et al. (2018) found no clear-cut dominance for the innovation distribution, although Gaussian and skewed-Gaussian distributions were among the best for most biofuel-related commodities. In this study, we retained an asymmetrical GARCH-based model with a Gaussian distribution and fundamental covariates both in the conditional variance and mean without

[2] According to Shapiro–Wilk and Jarque–Bera tests, price levels and differences are non-Gaussian, especially for daily data, whereas the augmented Dickey–Fuller (ADF), Phillips–Perron (PP), and Kwiatkowski–Phillips–Schmidt–Shin (KPSS) stationarity tests clearly confirm that these time series are integrated of order 1. We also found no statistically significant seasonality.

structural changes so as to simplify multivariate estimations and interpretation of empirical results. Moreover, we constrained the upper left-hand elements of matrices A, B, and D to be strictly positive to ensure identification of model parameters (Hafner & Herwartz, 1998). Additionally, to ensure covariance stationarity, all the moduli of the eigenvalues of the matrix $(A \otimes A)^{\tau} + (B \otimes B)^{\tau} + 1/2(D \otimes D)^{\tau}$ must be less than 1 (as shown in Appendix B).

We used the maximum likelihood two-step method to estimate our model, with the estimation of the conditional mean model followed by the conditional volatility model that we apply to the residuals.[3]

In line with the report of Abdelradi and Serra (2015), we encountered convergence issues[4] while trying to estimate each model using a standard quasi-Newton method, namely the Broyden–Fletcher–Goldfarb–Shanno (BFGS) algorithm. To solve this problem, we chose an alternative method, which was initially proposed by Demos and Sentana (1998), and this involves first refining the initial parameter proposals using several estimations based on the simplex method (Murty, 1983) and then switching back to the BFGS algorithm.[5] We thus obtain the Hessian matrix, which enables the calculation of standard errors for each estimated parameter, and then we derive the significance of each parameter combination in the conditional variance equations.

2.2 Price-level analysis

To better understand the causality relationships among vegetable oils, in our empirical study, we first carry out an analysis of the price discovery process. This analysis determines which, if any, vegetable oils lead the others, and it was recently applied to agricultural commodities markets by Adämmer and Bohl (2018) and Vollmer et al. (2020). We use the permanent–transitory (PT) measure,[6] introduced by Schwarz and Szakmary (1994) and formalised by Gonzalo and Granger (1995), for which the number of common factors driving prices will depend on the cointegration rank r and the number of cointegrated prices K: $K - r$. Gonzalo and Granger (1995) showed that P_t^P, the permanent component driving prices in the long run, can be expressed as a linear combination of the cointegrated prices when respective weights are orthogonal to the mean reversion coefficient α in equation (1), such that: $P_t^P = \alpha_{\perp} P_t$, and $\alpha_{\perp}^{\tau}\alpha = 0$.[7] $PT_{i,j}$ measures the contribution of the vegetable oil price i to the common factor j ($1 \leq i \leq K$ and $1 \leq j \leq K - r$), with $\alpha_{\perp}^{i,j}$ denoting the element in the i-th row and j-th column of $\alpha_{\perp}$:

$$PT_{i,j} = \frac{|\alpha_{\perp}^{i,j}|}{\sum_{k=1}^{K} |\alpha_{\perp}^{k,j}|} \tag{2}$$

This analysis is subsequently complemented with the study of price impulse response functions (IRFs), which tell us how each vegetable oil price will react and absorb an exogenous shock

[3] The two-step approach is very standard in the literature and leads to negligible differences from a one-step estimation when assuming a Gaussian distribution (Lütkepohl, 2005).

[4] We used the TsDyn package of R to estimate our VECM, and then the GARCH instruction of WinRATS (Estima) to estimate our BEKK–GJR–MGARCH model, which is the most developed and optimized software package for all GARCH-based models.

[5] The Berndt–Hall–Hall–Hausman (BHHH) algorithm can be considered when the BFGS method is not converging.

[6] Vollmer et al. (2020) also used the information share (IS) of Hasbrouck (1995) and the information leadership share (ILS) of Yan and Zivot (2010) and Putniņš (2013). However, these price discovery measures require only one common factor ($r = K - 1$), and they restrict the form of the cointegrating vector to $\beta = [1_{K-1}, I_{K-1}]^{\tau}$, in which 1_{K-1} is a column vector of 1 and I_{K-1} is the identity matrix, to obtain the orthogonal vector of β in the form $\beta_{\perp} = 1_K$. These measures are therefore not applicable in our paper.

[7] We used the orthogonalisation method proposed by Gonzalo and Ng (2001), which consists in taking the eigenvectors associated with the $K - r$ smallest eigenvalues of $\alpha\alpha^{\tau}$.

over time. Following Lütkepohl (2005), we developed the IRF of a unit shock (standard deviation) on standardised VECM–BEKK–GJR–MGARCH residuals to obtain uncorrelated price residuals ($\zeta_t \sim \mathcal{N}(0, I_K)$) and to remove the ARCH effects of ε_t, which significantly improves the IRF efficiency.

2.3 Variance–covariance analysis

To avoid any hazardous interpretation of the estimated parameters of the multivariate GARCH models, it is recommended that the conditional variance equation is derived along with the p-values associated with each explanatory variable (a detailed derivation is provided in Appendix C). However, the presence of cross-product terms with exogenous variables renders the analysis of their marginal impact on the vegetable oil variances and covariances difficult. This is why, following Serra and Gil (2013) and Abdelradi and Serra (2015), we derived the marginal effects of each exogenous variable as:

$$\frac{\partial(\Sigma_{t|t-1})_{ij}}{\partial z_{s,t}} = \sum_{k=1}^{\min(i,j)} (C^G_{z_s})_{jk}(C^G_t)_{ik} + (C^G_{z_s})_{ik}(C^G_t)_{jk} \tag{3}$$

Furthermore, this marginal contribution is combined with a volatility IRF (VIRF) to fully capture the dynamics of the vegetable oil price volatility dependence structure. The objective is first and foremost to quantify the impact of a shock at a given time t on all the conditional variances and covariances. With this VIRF, we also aim to assess the persistence of a shock; in other words, we aim to determine how the shock will be absorbed by the different variables over time. To this end, two methods are considered: the VIRF developed by Hafner and Herwartz (2006) and the conditional volatility profiles developed by Gallant et al. (1993).

Hafner and Herwartz (2006) define the MGARCH VIRF as the difference between the expected conditional variance–covariance matrix given an initial state and price shock ζ_t, and the expectation given the history:

$$V_h(\zeta_t, \mathcal{F}_{t-1}) = E[\text{vech}(\Sigma_{t+h|t+h-1})|\mathcal{F}_{t-1}, \zeta_t] - E[\text{vech}(\Sigma_{t+h|t+h-1})|\mathcal{F}_{t-1}] \tag{4}$$

While the authors provide the formula for the standard MGARCH, we contribute to this literature by deriving in Appendix D the analytical expression associated with the asymmetric MGARCH VIRF. To do this, we consider the MGARCH in its vech form, with D_K the duplication matrix of a $(K \times K)$-symmetric matrix and D_K^+ its Moore–Penrose inverse. We note the associated elimination matrix L_K to obtain the expression:

$$\begin{aligned} V_1(\zeta_t, \mathcal{F}_{t-1}) = {} & A^{\text{vech}} D_K^+ (\Sigma^{1/2}_{t|t-1} \otimes \Sigma^{1/2}_{t|t-1}) D_K \,\text{vech}(\zeta_t\zeta_t^\tau - I_K) \\ & - D^{\text{vech}} D_K^+ \Big[\Big[\text{diag}\left\{\mathbb{1}_{x>0}(\Sigma^{1/2}_{t|t-1}\zeta_t)\right\} \Sigma^{1/2}_{t|t-1}\Big] \otimes \\ & \Big[\text{diag}\left\{\mathbb{1}_{x>0}(\Sigma^{1/2}_{t|t-1}\zeta_t)\right\} \Sigma^{1/2}_{t|t-1}\Big] \Big] D_K \,\text{vech}(\zeta_t\zeta_t^\tau - {}^1\!/_2 I_K) \\ V_h(\zeta_t, \mathcal{F}_{t-1}) = {} & (A^{\text{vech}} + B^{\text{vech}} + {}^1\!/_2 D^{\text{vech}})^{h-1} V_1(\zeta_t, \mathcal{F}_{t-1}) \qquad \text{for } h > 1 \end{aligned} \tag{5}$$

where:

$$\begin{cases} A^{\text{vech}} & = D_K^+ (A \otimes A)^\tau D_K \\ B^{\text{vech}} & = D_K^+ (B \otimes B)^\tau D_K \\ D^{\text{vech}} & = D_K^+ (D \otimes D)^\tau D_K \end{cases} \tag{6}$$

While Hafner and Herwartz (2006) considered a fixed or a random initial shock and state, historical shocks could also be used, as proposed by Hassouneh et al. (2017). For the purpose of

our study, we decided to consider a random shock, with $\zeta_t \sim \mathcal{N}(0, I_K)$, and, to avoid arbitrarily fixing our initial state, we simulate 10^3 random shocks for each historical state observed in our data set. We then graphically represent the 5th and 95th percentiles associated with the related shock impact distributions.

As a complementary analysis, we study the volatility impulse response function following the conditional volatility profiles method proposed by Gallant et al. (1993) and apply it to the asymmetric MGARCH model, as detailed in Appendix E. This approach involves measuring the difference between the variance–covariance matrix forecasts with and without a given shock δ to the system at time t and averaging it over t such that:

$$\Phi_{\cdot,h}(\delta) = \frac{1}{T-1} \sum_{t=2}^{T} \widehat{\Sigma}^{\delta}_{t+h|t} - \widehat{\Sigma}_{t+h|t} \tag{7}$$

Finally, we investigate the extent to which the volatility of an asset could spill over into the volatility or the covariance associated with the other assets. The 'volatility spillover' measure proposed by Diebold and Yilmaz (2009) relies on the forecast error variance decomposition (FEVD) of a VAR model. Diebold and Yilmaz (2012) developed this concept of directional spillovers to assess how much the variance of each asset propagates towards the variance of other assets, and inversely how much they receive from the variances of other assets. To override the limitations of rolling-window methods, such as their lack of heteroscedasticity, Fengler and Herwartz (2018) considered time-varying spillovers for the BEKK–MGARCH model without asymmetry. Here, we extend this last approach to the BEKK–GJR–MGARCH model, as detailed in Appendix F, wherein we also demonstrate the necessary conditions to ensure covariance stationarity for BEKK–GJR–MGARCH spillovers. For the one-step-ahead FEVD, the spectral radius of $\mathcal{A}_t = A^{\text{vech}} + B^{\text{vech}} + D_t^{\text{vech}}$ must be strictly less than 1, with:

$$D_t^{\text{vech}} = D_K^{+}(D \otimes D)^{\tau} \left[\text{diag}\left\{\mathbb{1}_{x>0}(\varepsilon_t)\right\} \otimes \text{diag}\left\{\mathbb{1}_{x>0}(\varepsilon_t)\right\}\right] D_K \tag{8}$$

We then estimate $\lambda_{t,ij}^{(H)}$, the proportion of the H-step-ahead forecast error variance of variable i attributable to innovations in variable j, and $\widehat{\Psi}_{t+H,h|t}$ is the impact of the h-step-ahead innovation to the H-step-ahead forecast error, with $0 \leq h < H$, such that:

$$\lambda_{t,ij}^{(H)} = \frac{\sum_{h=0}^{H-1} \left([\widehat{\Psi}_{t+H,h|t}]_{ij} \right)^2}{\sum_{h=0}^{H-1} \sum_{j=1}^{K^*} \left([\widehat{\Psi}_{t+H,h|t}]_{ij} \right)^2} \quad , \quad \text{with } \widehat{\Psi}_{t+H,h|t} = \widehat{\Theta}_{t+H-1,h|t} \widehat{\Omega}^{1/2}_{t+H-h|t} \tag{9}$$

where:

$$\begin{cases} \widehat{\Theta}_{t+H-1,0|t} & = I_{K^*} \\ \widehat{\Theta}_{t+H-1,1|t} & = A^{\text{vech}} + \mathbb{1}_{x=1}(H) D_t^{\text{vech}} + \mathbb{1}_{x>1}(H) 1/2 D^{\text{vech}} \\ \widehat{\Theta}_{t+H-1,h|t} & = (A^{\text{vech}} + B^{\text{vech}} + \mathbb{1}_{x=1}(H) D_t^{\text{vech}} + \mathbb{1}_{x>1}(H) 1/2 D^{\text{vech}}) \widehat{\Theta}_{t+H-1,h-1|t} \quad , \forall h > 1 \end{cases}$$

$$\widehat{\Omega}_{t+H-h|t} = L_K (\Sigma^{1/2}_{t+H-h|t} \otimes \Sigma^{1/2}_{t+H-h|t}) \widetilde{\Omega} (\Sigma^{1/2}_{t+H-h|t} \otimes \Sigma^{1/2}_{t+H-h|t}) L_K^{\tau} - \text{vech}(\Sigma_{t+H-h|t}) \, \text{vech}(\Sigma_{t+H-h|t})^{\tau}$$

where $\widetilde{\Omega}$ is the $(K^2 \times K^2)$-matrix collecting the fourth-order moments associated with ζ_t. We also derive $\mathcal{N}_{t,i}^{H}$, the net contribution of variable i to H-step-ahead volatility spillovers, which represents the difference in volatility transmitted to and received from the other variables. Following Fengler and Herwartz (2018), we further distinguish the spillovers between variances and covariances. We then define specific spillover indices for covariances and variances (own or cross); that is, $\mathcal{S}_t^{H,\text{ocov}}$ ($\mathcal{S}_t^{H,\text{ovar}}$), which represents the spillovers between all covariances

(variances), and $\mathcal{S}_t^{H,\text{ccov}}$ ($\mathcal{S}_t^{H,\text{cvar}}$), which represents the spillovers from covariances to variances (variances to covariances).

$$\mathcal{N}_{t,i}^{H} = \sum_{j=1;i\neq j}^{K^*} \frac{\lambda_{t,ji}^{(H)} - \lambda_{t,ij}^{(H)}}{K^*} \qquad \mathcal{S}_t^{H,\text{ocov}} = \sum_{i\in I_{\text{cov}}} \frac{\sum_{\substack{j\in I_{\text{cov}} \\ i\neq j}} \lambda_{t,ij}^{(H)}}{K^*} \qquad \mathcal{S}_t^{H,\text{ovar}} = \sum_{i\in I_{\text{var}}} \frac{\sum_{\substack{j\in I_{\text{var}} \\ i\neq j}} \lambda_{t,ij}^{(H)}}{K^*}$$

$$\mathcal{S}_t^{H,\text{ccov}} = \sum_{i\in I_{\text{var}}} \frac{\sum_{\substack{j\in I_{\text{cov}} \\ i\neq j}} \lambda_{t,ij}^{(H)}}{K^*} \qquad \mathcal{S}_t^{H,\text{cvar}} = \sum_{i\in I_{\text{cov}}} \frac{\sum_{\substack{j\in I_{\text{var}} \\ i\neq j}} \lambda_{t,ij}^{(H)}}{K^*}$$

where I_{var} and I_{cov} respectively embody the sets of variances and covariances.

3 Data description and model selection

3.1 Monthly and daily prices

In this study, we examined the dynamic price-dependence structure among the three major vegetable oils from January 2009 to December 2020. Sunflower oil (SFO), being the smallest market in terms of consumption (USDA, 2021) and also being much less used in non-food applications (Figure G1), has been omitted. Our monthly data were provided by Oilworld, and we chose the same origin (Netherlands) for the forward contracts to limit price adjustments due to logistic issues, and we used the free-on-board ex-mill prices.

For daily prices, again, we considered the same origin for the three vegetable oils to avoid discrepancies due to logistic issues. Furthermore, there is no futures market for RSO, and only over-the-counter (OTC) contracts are available. For these two reasons, we decided to work on OTC prices not only for RSO but also for SBO and PMO, although futures contracts are available for them in Chicago and Malaysia, respectively.[8] Reuters daily OTC prices are taken from brokers' surveys, but they suffer from structural limitations if the maturity of the contract is uncertain[9] and the price is an average mid-quote provided by several brokers without bid–ask size information. The data we considered were instead provided by one of the largest biofuel producers and RSO crushers in Europe. This unique database from January 2014 to December 2020 stands as a robust reference provided that the prices recorded on a daily basis by the company correspond to traded prices or brokers quotations (Figure G2).

Regarding covariates (Figure G3), we naturally considered the Brent crude oil price as a fossil energy benchmark, and the three-month Treasury bills rate and its six-month moving variance following Serra and Gil (2013), who suggest that the moving variance of interest rates could explain the volatility of corn and ethanol. These are also good indicators of global macroeconomic conditions. Furthermore, exchange rates can play an important role in triggering global import or export of oilseeds, and they therefore impact associated price dynamics (Abdelradi & Serra, 2015; Balcombe, 2011; Frank & Garcia, 2010). We thus retained the following foreign exchange rates: EUR/USD, USD/MYR (in which MYR is the Malaysian ringgit), and EUR/MYR.[10]

Finally, we added the United States Department of Agriculture (USDA) forecasts of stock-to-use ratios as they represent the supply and demand tensions for each vegetable oil. We also retained the forecasts of stock-to-use ratios associated with rapeseed and soybean seed, as crushing capacities have been continuously in excess since the 2000s. Stock-to-use ratio forecasts

[8] Both SBO and PMO OTC contracts are denominated in USD, whereas RSO OTC contracts are in EUR. For the sake of consistency, the RSO contracts have been converted in USD using the prevailing three-month forward exchange rate.

[9] For historical data, Reuters only mentions if the price is associated with the first, second, or third maturity, but no maturity is clearly specified, and this thus leads to misleading price jumps

[10] EUR/MYR is calculated from EUR/USD and USD/MYR, and we only include two of them when our model selection pre-processing recommends them all.

were calculated as ratios between the given commodity forecasted level of global ending stocks and its related consumption expected by the USDA. In the literature, Serra and Gil (2013) pointed out that a high ratio reduces corn price volatility, whereas Abdelradi and Serra (2015) showed that an increase in RSO inventories could lead to reductions in the price volatility of both RSO and biodiesel. Each exogenous variable is considered both in level and first difference.

3.2 Model selection

We first studied the stationarity of the time series by running the ADF unit-root test and the PP and KPSS stationarity tests. These confirmed that the log-prices of the three vegetable oils are $I(1)$[11] (Table A1). Then, to test for cointegration relationships, we retained the BIC to specify the lag, the deterministic component of the cointegrating space, and the rank of the cointegrating vector. Table A2 indicates that both daily and monthly prices have a cointegration rank $r = 1$. The choice of no deterministic term was stipulated for all samples. We verified these results with Johansen cointegration tests in Table A3, and we validated our hypothesis at 5% statistical significance for the monthly sample and 1% significance for the daily sample (Johansen, 1991). Moreover, to determine which exogenous variables to retain, we considered the standard stepwise method using the Akaike information criterion (AIC). With this sequential method, we selected only the covariates for which the likelihood marginal contribution was significant and rejected the others.[12]

Regarding the frequency of the data, when we checked the parsimony of the daily and monthly models,[13] the daily model turned out to be parsimonious, whereas for monthly data, the addition of the conditional variance dynamics did not make a significant contribution. It indeed appears that more information about the price dynamics of the assets can be extracted from the daily data set, especially when studying the volatility dependence structure, which is quite intuitive. Furthermore, unlike some reports in the literature (Balcombe, 2011; Cha & Bae, 2011; Cooke, 2009; Hassouneh et al., 2017; Qiu et al., 2012; Serra & Gil, 2013), we found that the USDA's forecasts of stock-to-use ratios, which represent the tension between anticipated supply and demand, do not impact the monthly price levels, nor their volatility. However, they have strong effects on daily price volatility. This confirms the importance of using high-frequency data to study asset price volatility (Andersen et al., 2003).

4 Analysis of results

First, we will analyse price dynamics and the price discovery process, and then we will consider the dynamics of price volatility. Thereafter, the effects of covariates will be studied.

4.1 Substitutability and complementarity in EU vegetable oil markets

To fully understand the interactions among vegetable oils resulting from biodiesel production, the CFPP is a crucial variable to consider. First, it is worth noting that each vegetable oil can be esterified to produce biodiesel; after esterification, RSO, SBO, and PMO will respectively become rapeseed methyl ester (RME), soybean methyl ester (SME), and palm methyl ester (PME). However, each vegetable methyl ester has a specific CFPP: for RME this is -14°C, for SME it is -2°C, and for PME it is $+11$°C. Biodiesel producers then have the possibility of

[11] Lags used for these tests were determined with the Bayesian information criterion (BIC), which is a strongly consistent criterion.

[12] Full details about the stepwise log-likelihood results are provided in Appendix A.

[13] We determined whether the addition of the conditional variance dynamics was statistically relevant using log-likelihood ratio tests (see the results in Table A5).

blending these vegetable methyl esters to produce fatty acid methyl ester (FAME) for biodiesel. The CFPP of this blend will be a weighted average of the constituent vegetable methyl ester CFPP values.

This technical parameter is extremely important for biodiesel consumption, as it must be below the ambient temperature where the biodiesel is used. As a consequence, depending on the season and the location it is consumed, the biodiesels produced in Europe may have different CFPP values and thus be the result of different blends. For instance, a biodiesel with a CFPP of 0°C prevails in Europe over the summer (we will refer to this as FAME 0), whereas over cold periods such as winter in France, FAME −5 is produced. Said differently, the weighted average CFPP of the resulting vegetable oil blend should be below −5°C. Being significantly colder, the winters of European Nordic countries require a FAME −10 blend, and this is mainly made from RME. Producing an out-of-spec biodiesel with too high a CFPP can be very costly for an energy company, as it entails the loss of contracts and cumbersome inventories.

In this context, being the vegetable oil with the lowest CFPP, RSO is essential in this industry from maintaining a CFPP below the maximum level initially contracted with a client. That being said, RSO is also one of the most – if not *the* most – expensive vegetable oils, which explains why other vegetable oils may also be considered for biodiesel production.

There is another important point that should be emphasised: both the CFPP and the global production volumes for each vegetable oil are expected to play key roles in the substitutability and complementarity among vegetable oils, and they will hence have an impact on the joint dynamics of the associated market prices. For instance, RSO and SBO are good substitutes; this is in contrast to PMO, which is penalised by its high CFPP. European countries, being important producers of low-CFPP rapeseed, generally consider the high-CFPP but cheap PMO as an interesting complement for biodiesel production. This is confirmed by the fact that RSO represents 43% of the vegetable oil volume used by European biodiesel producers; PMO accounts for 29%, while SBO represents only 5% (Table G1).

By way of contrast, the United States and South American countries (in particular Brazil and Argentina) do not have CFPP constraints. They do, however, have to report the cloud point (CP) of the produced biodiesel, another low-temperature property; this corresponds to the temperature at which small crystals will form in the biodiesel. SME and RME have an almost identical CP, respectively 1°C and 0°C, while the value is 17°C for PME (Moser, 2008). Moreover, soybean is one of the main crops in these countries, and this explains the large dominance of SBO (almost 90% of biodiesel is produced from SBO) while RSO and PMO are mainly considered for economic reasons, especially in the US.

These specificities of the vegetable oil market are captured and quantified by our model. As shown in Table 1, the cointegration rank being one, two common factors should be carved out in our price discovery analysis. Interestingly enough, the second principal component shows a clear dual relationship between the European prices of RSO and PMO, and we could link this to the European biodiesel market structure we described earlier. Furthermore, the other factor embodies instead the American market structure, with a predominance of SBO versus the two substitutable vegetable oils.

Another interesting point to make is the alternating signs displayed in the cointegrating vector. We indeed observe that RSO and PMO both have a positive sign, which is in contrast to SBO; this shows the complementarity of RSO and PMO and their substitutability with SBO. Our results thus demonstrate that vegetable oil market prices are mainly driven by the long-term blending intentions of biodiesel companies as well as the structural agronomic specificities associated with the producing regions.

	PT_1	PT_2
RSO	25%	42%
SBO	55%	0%
PMO	19%	58%

$$\text{RSO} + 1.139^{***}\text{PMO} = 2.110^{***}\text{SBO}$$

Table 1: Price discovery and cointegrating vector
Note: *** indicates statistical significance at the 1% level.

4.2 Covariance contagion and variance spillover

We now investigate how a supply or demand shock on one of the vegetable oils propagates to another. Although the long-term cointegration relationship turns out, as demonstrated above, to be the main price-transmission channel, the joint sensitivities of the variances and covariances of vegetable oils constitute another important vector of connectedness in commodities markets. Furthermore, the speed with which the shocks can be absorbed is extremely relevant for the industry to design appropriate hedging solutions.

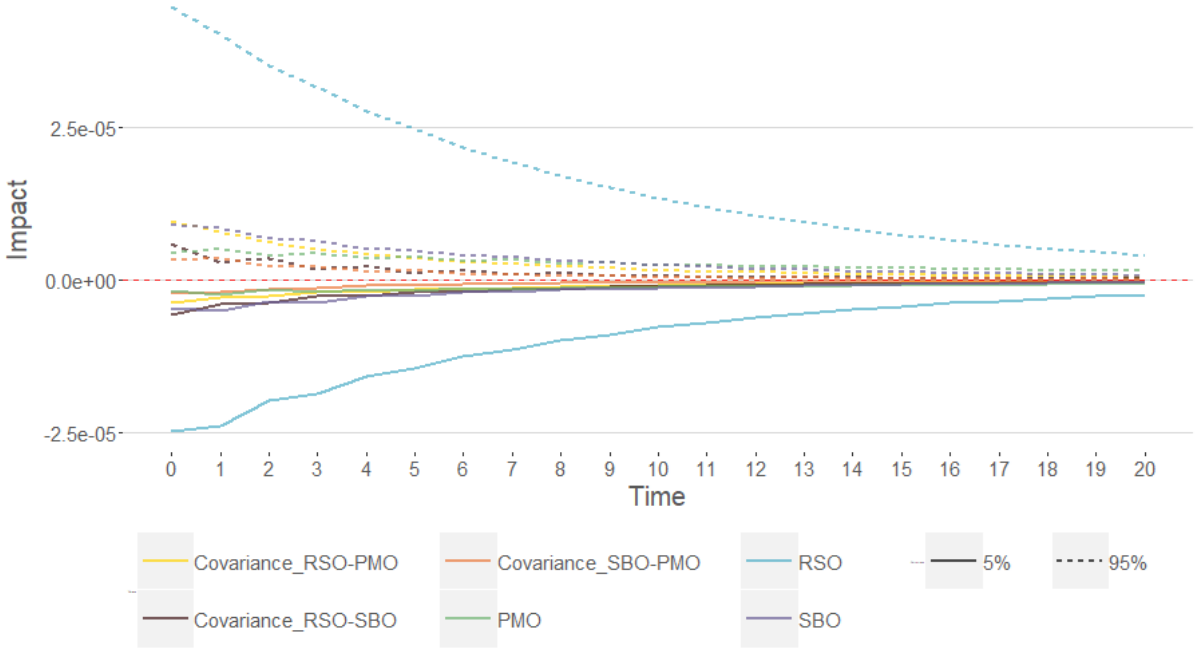

Figure 1: Daily volatility impulse response function (price shocks).

Regarding the asymmetric effects of price shocks, Figure 1 clearly shows that positive price shocks increase price volatility twice as much as negative price shocks. Furthermore, this phenomenon is much more pronounced on the RSO market, where daily price shocks take more than a month to be fully absorbed. One possible explanation for this is that RSO, being the only vegetable oil among the three without a futures market, is more sensitive to price shocks, and this tends to amplify its effect on the economy through higher volatility over a longer period of time. As market operators have no access to a liquid hedging product, they need much more time to adjust their positions.

Additionally, Figure 2 tends to show that the main vegetable oil used by the European biofuel industry, RSO, is a recipient of stress in the other vegetable oil markets. We can indeed notice that PMO and – to a lesser extent – SBO variances spill over into RSO volatility as

well as all the covariances among these vegetable oils. As such, the trade war between the United States and China early in 2018 noticeably spread out on the RSO market, creating tensions on this market, whereas PMO was less impacted (Marchant & Wang, 2018). Once again, RSO being less liquid serves as an adjustment variable and experiences shocks from the other vegetable oil markets. The volatility of the European market is thus driven by the US and Indonesian markets, which are much larger and more liquid.

Another interesting point to make is the significantly stronger spillover effect from variances towards covariances relative to covariances towards variances, covariances towards covariances, or variances towards variance spillovers.[14] Therefore, a volatility shock (especially to PMO or SBO) will significantly increase the covariance among vegetable oils, and this will thus amplify the connectedness of the vegetable oil markets. This will similarly reduce the efficiency of the hedging strategies of biodiesel producers that are based on vegetable oil exposure diversification.

Regarding the price volatility contagion mechanism, these results demonstrate that the price volatilities of vegetable oils do not directly impact each other. Tensions in a particular vegetable oil market will first impact covariances between vegetable oil prices, and only then will this affect the other vegetable oils' variances. This connectedness among markets, conditionally upon the filtration generated by the set of explanatory variables, echoes the results of Bekaert et al. (2005), as it is not explained by fundamental factors (the fundamental variables are treated as being fixed in the calculation of spillover indices) but instead by trader activities and potentially the fact that biodiesel producers cannot hedge their exposure on RSO via futures. The inertia in factory blending decisions thus entails an unhedgeable risk on RSO, leading to frictions that are then reflected in the joint dynamics of market price volatilities.

4.3 Energy price shocks and other macroeconomic variables

Beyond a demand or supply shock on one of the vegetable oil markets, other exogenous variables influence their joint price dynamics and thus the production cost of biofuel. Among these, we notice that Brent price fluctuations have a significant positive impact on all vegetable oil prices (see Table 2). Therefore, a rise in the Brent price leads to increases in all vegetable oil prices, a phenomenon that we observe in the current post-COVID environment. Furthermore, this result sheds light on the contradictory literature about the relationship between agricultural and energy prices (Myers et al., 2014; Paris, 2018; Sanders et al., 2014; Serra & Zilberman, 2013). Our unambiguous positive relationship between vegetable oil prices and the Brent price is certainly due to the fact that we are working directly with the prices of vegetable oils instead of the prices of vegetable seeds, as has been the approach in many other studies. Likewise, Zhen et al. (2018) demonstrated that in the Canadian cattle market, volatility transmission does not pass through more than one level within the supply chain. One should also note that the Brent sensitivity is slightly stronger for SBO, which is by far the most liquid market and thus may be more prone to food-versus-energy relative-value trading strategies.

To get a better grasp of this relationships between vegetable oils and the energy market, we propose to study the impact of a Brent price shock through the IRF. Figure 3 shows that a Brent price increase will lead to a rise in vegetable oil prices. However, the IRF also informs us about the persistence of this shock, which is crucial for inflation targeting. Our empirical results show that a temporary shock in the Brent price is absorbed by the vegetable oil daily prices in only around six days. This relatively short duration demonstrates the capacity of vegetable

[14] We note the high volatility and heteroscedasticity of these spillover indices. It is worth mentioning that if we had used the Diebold and Yilmaz (2012) rolling-window method for the same plot, only representing the average spillover rate on the considered window instead of the spillover rate at time t, we would have missed this information.

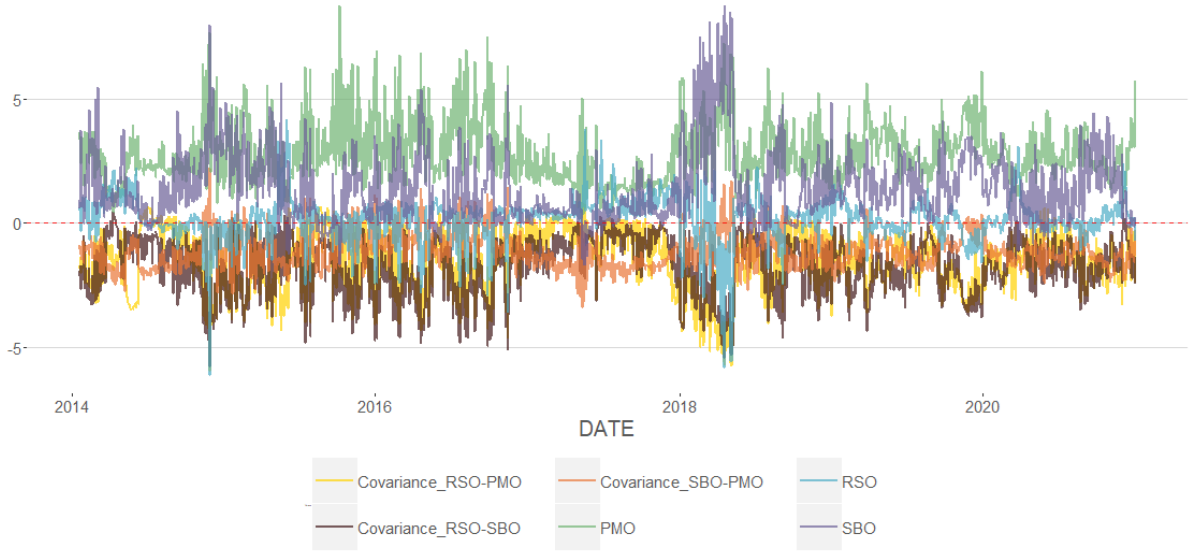

(a) Net spillover indexes.

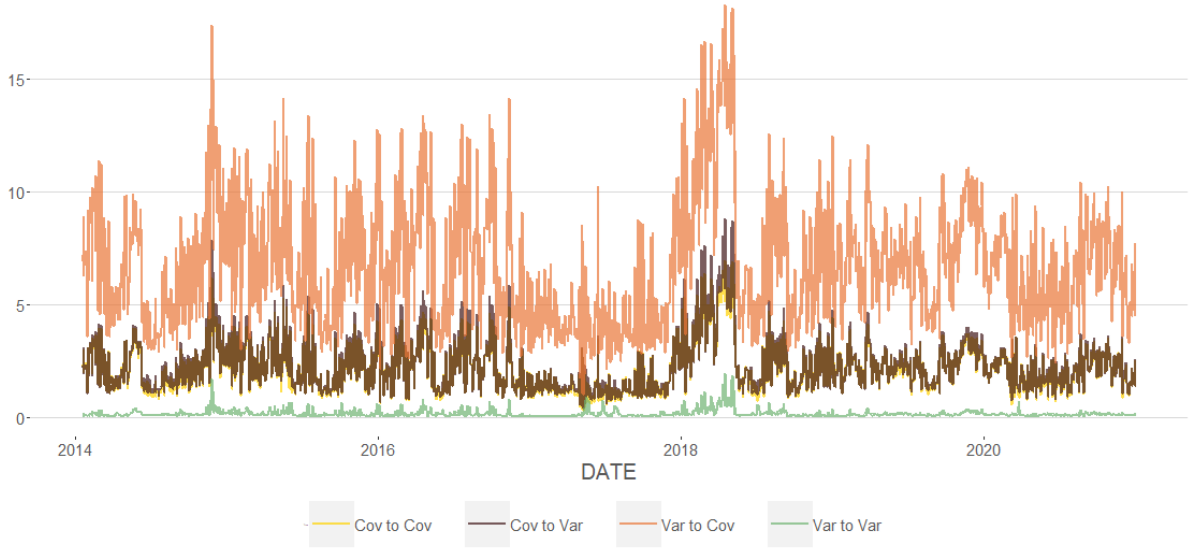

(b) Own/cross (co)variance spillovers.

Figure 2: Net spillover index and own/cross (co)variance spillovers.

Note: For each sample, this figure represents the evolution of the own or cross variance–covariance spillovers, and the evolution of $\mathcal{N}_{t,i}^{H}$, the net contribution of each variable. We used $H = 5$ because with $H > 3$, the figures are very similar whatever the H-step ahead used (other figures are available upon request).

oil markets to efficiently revert to equilibrium price following a sudden burst or collapse of the energy market.

Contrary to these fairly unambiguous relationships between the trend components of vegetable oils and Brent, its impact on their stochastic variance and covariances is not as clear-cut.[15] As shown in Table 2, the exchange rate fluctuations also have a clear impact on vegetable oil

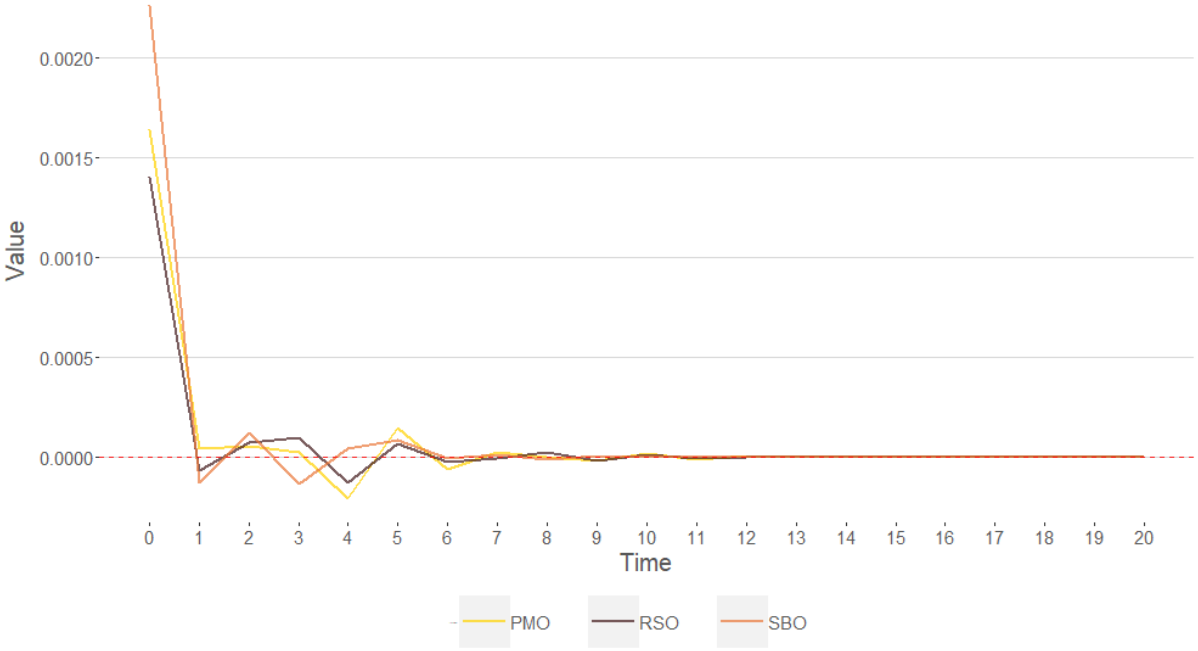

Figure 3: Price impulse response function after a Brent price shock.

prices. For instance, the EUR/USD exchange rate variations have a positive impact on all vegetable oil prices. With regard to RSO, this relationship comes from the fact that the RSO OTC products considered for this study are initially quoted in EUR and we converted them into USD for the sake of comparison. As a consequence, when EUR is appreciating against USD, the price of RSO in USD will increase. Conversely, SBO is initially quoted in USD, so the strong positive link we observe results from the SBO depreciation in EUR when the EUR/USD exchange rate is rising. Compared to the other vegetable oils, this depreciation makes RSO more interesting to purchase for European biofuel producers, which thus entails a stronger demand. The very same reasoning can be applied to PMO, which is quoted in USD.

In contrast, the USD/MYR exchange rate variations have a negative impact on vegetable oils, especially on PMO, which is twice as strong as its impact on SBO prices. The PMO futures market in Malaysia quotes in MYR, and as the largest worldwide market for PMO, it generally leads the Rotterdam market, where the PMO OTC products are denominated in USD. As such, if we assume that the PMO Malaysian price remains unchanged while the USD/MYR exchange rate is rising, the PMO Rotterdam price converted into USD can consequently be expected to drop. Moreover, the negative effect of the USD/MYR on SBO is interesting as it illustrates European traders' decisions to substitute SBO with PMO. They indeed favour PMO over SBO when the Rotterdam PMO USD-equivalent price decreases due to devaluation of MYR against USD. As our analysis encompasses the three main vegetable oils used for biofuel production –

[15] Figure H1 shows that a rise in the Brent price does seem to decrease SBO variance and increase PMO variance, but only to a very limited extent. The magnitude of this impact is indeed of order 10^{-7}, whereas the average daily variation of variance is of order 10^{-5}.

unlike Abdelradi and Serra (2015) who focused on RSO – it sheds light on the substitutability phenomenon among vegetable oils that is associated with exchange rate fluctuations.

	DIFFERENCE				
	Brent	EURUSD	USDMYR	Ratio SBO	Ratio PMO
RSO	1.70E−4***	0.709***	−0.014	0.107	−0.006
SBO	2.74E−4***	0.129***	−0.042**	0.014	0.059**
PMO	1.98E−4***	0.195***	−0.108***	−0.258*	0.049

Table 2: VECM significative exogenous variable parameters – daily.
Note: *, **, and *** indicate statistical significance at the 10%, 5%, and 1% levels, respectively.

The significance of exchange rates in explaining part of the price volatility in agricultural commodities has already been demonstrated by Balcombe (2011) and Abdelradi and Serra (2015). However, their impact on vegetable oil covariances has not yet been demonstrated. The results displayed in Table 3 contribute to the literature in this respect and show that depreciation of both the US dollar and the Malaysian ringgit will put pressure on RSO, leading to it becoming the most expensive oil and thus translating into higher volatility. Substitution strategies then take place, and these result in a decrease of the covariances between RSO and PMO when MYR depreciates and between RSO and SBO when the US dollar depreciates.[16]

4.4 Storage theory and conditional variance

Unlike most of the related literature (Carter et al., 2012; Cooke, 2009; Gilbert, 2010; Hassouneh et al., 2017; Headey & Fan, 2008; Hochman et al., 2011; Kim & Chavas, 2002; Meyers & Meyer, 2008; Mitchell, 2008; Shively, 1996; Wright, 2011), we found that the anticipated stock-to-use ratio has no effect on the monthly vegetable oil price, nor on the monthly conditional variances and covariances, and it only has a limited impact on the daily price momentum. However, we notice a salient effect of vegetable oils and seed inventories on the conditional variances and covariances of the vegetable oil daily prices. This validates the well-documented storage theory in a daily-frequency framework and extends it to the covariances among goods.

Before analysing our results regarding the price momentum, we need to explain the link between inventories and prices for both substitutable and complementary goods. In the context of a single commodity market, the economic theory of storage states that the price of a commodity will be negatively correlated with its own supply; i.e., if the stocks of a commodity decrease, then the price of that commodity should increase. In a two-commodity setting, Casassus et al. (2013) define the relationship of two products as complementary if 'they share a balanced supply or are complementary in either consumption or production'. For consumption-complementary goods, this means that for a given increase in demand for one of the products, both products will be simultaneously consumed, thus leading to price increases for both of them. However, in the case of substitutable goods, higher demand for one product will be offset by a contraction of the other product consumption. Thus the first good inventories decrease and its price increases, while the second good inventories increase and its price decreases.

Knowing this, when we look at Table 2, the 'Ratio PMO' associated column shows us a significant substitution effect between PMO and SBO (a higher PMO stock-to-use ratio,

[16]While not significant for the trend component, the Treasury bills variance turns out to be of importance as far as the conditional variance is concerned. Its influence is positive on all the variances as well as the SBO–PMO covariance (see Table 3); this can be interpreted as a positive influence on vegetable oil volatility from central bank policy uncertainty, and this is associated with inflation and economic growth forecasts. This phenomenon has also been pointed out by Serra and Gil (2013) on the US corn market.

meaning higher PMO supply or lower PMO demand, leads to a higher SBO price). However, the 'Ratio SBO' column shows us instead that SBO and PMO turn out to be complementary goods (a higher SBO stock-to-use ratio leads to a lower PMO price). This presumed contradiction can be justified by the fact that the SBO inventories depend mainly on the decisions of US biofuel producers rather than EU biofuel producers, as US biofuel producers use almost five times more SBO to produce biodiesel than EU producers. As explained in subsection 4.1, the US does not have a CFPP constraint, and therefore the SBO/PMO complementarity observed in the US biofuel market, due to economic reasons, impacts PMO prices. Conversely, European biodiesel producers first favour their own RSO and then substitute between PMO and SBO to reach a given CFPP, which explains the SBO/PMO substitutability characterising the European biofuel market.[17]

	LEVELS								DIFFERENCES		
	Brent	VM Tbills	USDMYR	Ratio RSO	Ratio SBO	Ratio SFO	Ratio RS	Ratio SB	EURUSD	EURMYR	Ratio SFO
Var RSO	−8.49E−09	7.34E−03	1.67E−05	1.50E−04	1.89E−04	−1.46E−04	−2.38E−04	1.24E−04	5.89E−04	1.25E−04	−3.70E−04
Var SBO	−4.82E−08	1.88E−03	−1.83E−05	2.57E−04	−1.73E−04	−3.89E−04	1.33E−04	1.44E−04	−1.49E−03	1.42E−04	4.25E−04
Var PMO	4.50E−08	3.24E−03	3.84E−06	4.63E−05	4.29E−04	−1.82E−04	−1.41E−04	6.56E−05	−1.76E−04	4.40E−05	1.85E−04
Cov RSO–SBO	−1.82E−08	5.85E−03	5.97E−06	2.17E−04	1.64E−04	−2.59E−04	−1.14E−04	1.46E−04	−1.07E−04	1.36E−04	−5.23E−05
Cov RSO–PMO	−7.87E−09	2.36E−03	−1.74E−06	6.36E−05	−9.66E−05	−8.90E−05	−4.69E−05	4.44E−05	−1.31E−05	1.21E−05	−8.56E−05
Cov SBO–PMO	4.28E−10	2.04E−03	−4.01E−06	1.64E−04	1.44E−04	−1.85E−04	2.25E−05	8.22E−05	−1.48E−04	−1.30E−05	1.88E−04

Table 3: Marginal effects

Note: Based on Table C1 we determine on which variances or covariances each exogenous variable combination has a statistically significant impact. We then qualify as significant first-order exogenous variables those that have a statistically significant impact via their level, while the significant second-order exogenous variables are those with a statistically significant impact through their squared value. Table 3 then provides us the marginal impact of each exogenous variable at the data means over the entire sample studied. Values with a green or a yellow background indicate significant first- or second-order exogenous variables, respectively.

Regarding the relationship between the price covariance and the stock-to-use ratio, price changes of commodities sharing a complementary relationship are positively correlated following a positive shock to the relative scarcity of one of them, which means that the covariance between the two commodities increases. Conversely, the prices of products sharing a substitution relationship are negatively correlated following a positive shock to the relative scarcity of one of them, which means that the covariance between the two products decreases. The econometric model used in our paper tells us whether the covariances between products are stronger or weaker when the relative availability of a product is high or low. Moreover, according to the very rich literature on the economic theory of storage, when forecasted stock-to-use ratios are increasing, the price volatility of the associated goods should be lower (Abdelradi & Serra, 2015; Balcombe, 2011; Kim & Chavas, 2002; Serra & Gil, 2013; Shively, 1996; Stigler & Prakash, 2011; Williams, Wright, et al., 2005; Wright, 2011). If one product shares a complementary relationship with another, then an increase in the relative scarcity of the first will lead to an increase in the volatility of both products, as prices will react in the same way to a change in the relative scarcity of either of the products. However, if this other product instead shares a substitution relationship, then an increase in the relative scarcity of the first product will lead to a decrease of the volatility of the second product, as prices react in the opposite way to a change in the relative scarcity of one of the products.

From an empirical perspective, it is worth reiterating that European crushing capacities have always been in excess. Therefore, when a stock of oilseeds is available, an increase in the crushing throughput entails a higher inventory of the associated vegetable oil. The oilseed inventories could thus be considered as secondary inventories for the associated vegetable oils.

[17] Another large consumer of PMO to produce biodiesel is Indonesia, but they do not blend it with other vegetable oils and thus could not have any marginal effect on the vegetable oil complementarity or substitutability.

It is therefore appropriate to jointly consider the stock-to-use ratio coefficients associated with oilseeds and those associated with vegetable oils.

As we analyse our empirical results, we can see that Table 3 verifies the storage theory. The relative scarcity of rapeseed (measured as the combination of 'Ratio RS' and 'Ratio RSO') indeed has a positive impact on the RSO variance. Likewise, the relative scarcity of soybean (a combination of 'Ratio SB' and 'Ratio SBO') positively relates to the SBO variance. Moreover, according to our earlier argument, the combined rapeseed coefficients confirm its substitutability relationship with SBO (positive net impact of the rapeseed stock-to-use level on the SBO variance), and the complementarity relationship with PMO (negative net impact of the rapeseed stock-to-use level on the PMO variance). In like manner, the combined soybean coefficients highlight the substitutability relationship with RSO and PMO (positive impact). Interestingly enough, one can note that the covariances between RSO–SBO and SBO–PMO – i.e., covariances between vegetable oils that share a substitution relationship – are positively impacted by the relative availability of RSO and SBO.

Finally, the SFO stock-to-use ratio is statistically significant in level and in difference. It has a negative impact on the RSO variance, indicating a complementary relationship between RSO and SFO, and a positive impact on the SBO variance, showing a substitution relationship between SBO and SFO. The SFO ratio has no overall impact on the PMO variance, and we also note a negative effect on the RSO–SBO covariance. These relationships are derived from food uses, as SFO is used almost exclusively for this purpose (Figure G1). Europe has very inelastic demand, the quality, and label constraints indeed cause food companies to use mostly non-GM RSO or SFO, and whatever their price, they do not change the vegetable oil used. This explains the complementary relationship between RSO and SFO: an increase in food demand will generate an increase in demand for both RSO and SFO. In contrast, Table G1 indicates that SBO is much less used in Europe for non-biodiesel uses. The substitution relationship between SBO and SFO is mainly due to the price-oriented import policies of Asian countries, which import SBO or SFO largely according to their price because they have far fewer constraints than Europeans. We also note a negative effect on the RSO–SBO covariance.

5 Conclusion

Motivated by the recent evolution of food and energy prices, we used a VECM–BEKK–GJR–MGARCH model to jointly examine price and volatility dynamics characterising the three main vegetable oils involved in EU biofuel production. Our analysis further included macroeconomic factors for each vegetable oil's conditional mean, variance, and covariances.

We applied our model to monthly and daily prices using a unique data set provided by a major European crushing company and biodiesel producer. The two sets of results significantly differ in their economic interpretation and variance dynamics. Unlike most of the literature, we found that the USDA's forecasts of stock-to-use ratios, representing the expected tensions between supply and demand, do not impact monthly prices, nor do they impact their associated volatility. However, we found that they have significant effects on daily price volatility.

We also contribute to the literature by highlighting and assessing the effects of vegetable oil substitutability and complementarity on prices. While RSO and SBO are good substitutes, this is not the case for PMO. In Europe, PMO is complementary to RSO for biodiesel blending. This stems from its industrial technical parameters, especially the CFPP. This distinction between substitutability and complementarity is essential and explains the different results and causality structures we retrieved through market price levels and dynamic analysis of volatilities, for example the fact that RSO and SBO are the main drivers of vegetable oil prices. We also showed that, through the Brent price, the energy market has only a positive influence on vegetable oil

price levels, but it has no influence on their volatility. In the same vein, it is interesting to note that exchange rates impact both price and volatility dependence structures, and they trigger substitution strategies among vegetable oils.

We demonstrated the existence of spillover effects on the European vegetable oil market at the daily frequency. The SBO and PMO variances constitute the major net contributors to these spillovers, while the RSO–SBO covariance stands as the major net receiver. From a practitioner point of view, and with regard to value-at-risk modelling, it is worth highlighting that spillover effects are mainly directed from variances towards covariances; they are also directed to a lesser extent from covariances towards variances, but also directly between covariances.

Finally, we contribute to the methodological literature by developing an analytical expression of the MGARCH VIRF with asymmetry, and we derived the necessary conditions to ensure covariance stationarity for spillovers when adding price volatility asymmetry and exogenous variables.

References

Abdelradi, F., & Serra, T. (2015). Food–energy nexus in Europe: Price volatility approach. *Energy Economics*, *48*, 157–167.

Adämmer, P., & Bohl, M. T. (2018). Price discovery dynamics in European agricultural markets. *Journal of Futures Markets*, *38*(5), 549–562.

Andersen, T. G., Bollerslev, T., Diebold, F. X., & Vega, C. (2003). Micro effects of macro announcements: Real-time price discovery in foreign exchange. *American economic review*, *93*(1), 38–62.

Balcombe, K. (2011). The nature and determinants of volatility in agricultural prices: An empirical study. *Safeguarding food security in volatile global markets*, 89–110.

Barbaglia, L., Croux, C., & Wilms, I. (2020). Volatility spillovers in commodity markets: A large t-vector autoregressive approach. *Energy Economics*, *85*, 104555.

Bekaert, G., Harvey, C. R., & Ng, A. (2005). Market integration and contagion. *The Journal of Business*, *78*, 39–70.

Carter, C., Rausser, G., & Smith, A. (2012). The effect of the us ethanol mandate on corn prices. *Working Paper. UC Davis, Davis, CA*.

Casassus, J., Liu, P., & Tang, K. (2013). Economic linkages, relative scarcity, and commodity futures returns. *The Review of Financial Studies*, *26*(5), 1324–1362.

Cha, K. S., & Bae, J. H. (2011). Dynamic impacts of high oil prices on the bioethanol and feedstock markets. *Energy policy*, *39*(2), 753–760.

Cheng, I.-H., & Xiong, W. (2014). Financialization of commodity markets. *Annu. Rev. Financ. Econ.*, *6*(1), 419–441.

Chkili, W., Hammoudeh, S., & Nguyen, D. K. (2014). Volatility forecasting and risk management for commodity markets in the presence of asymmetry and long memory. *Energy Economics*, *41*, 1–18.

Cooke, B. (2009). *Recent food prices movements: A time series analysis* (Vol. 942). International Food Policy Research Institute (IFPRI).

Demos, A., & Sentana, E. (1998). An EM algorithm for conditionally heteroscedastic factor models. *Journal of Business & Economic Statistics*, *16*(3), 357–361.

Diebold, F. X., & Yilmaz, K. (2009). Measuring financial asset return and volatility spillovers, with application to global equity markets. *The Economic Journal*, *119*(534), 158–171.

Diebold, F. X., & Yilmaz, K. (2012). Better to give than to receive: Predictive directional measurement of volatility spillovers. *International Journal of forecasting*, *28*(1), 57–66.

Engle, R. F., & Kroner, K. F. (1995). Multivariate simultaneous generalized ARCH. *Econometric Theory*, *11*, 122–150.

Fengler, M. R., & Herwartz, H. (2018). Measuring spot variance spillovers when (co) variances are time-varying : The case of multivariate GARCH models. *Oxford bulletin of economics and statistics*, *80*(1), 135–159.

Francq, C., & Thieu, L. Q. (2019). Qml inference for volatility models with covariates. *Econometric Theory*, *35*(1), 37–72.

Frank, J., & Garcia, P. (2010). How strong are the linkages among agricultural, oil, and exchange rate markets?

Gallant, R., Rossi, P., & Tauchen, G. (1993). Nonlinear dynamic structures. *Econometrica*, *61*, 871–907.

Gilbert, C. L. (2010). How to understand high food prices. *Journal of agricultural economics*, *61*(2), 398–425.

Gonzalo, J., & Granger, C. (1995). Estimation of common long-memory components in cointegrated systems. *Journal of Business & Economic Statistics*, *13*(1), 27–35.

Gonzalo, J., & Ng, S. (2001). A systematic framework for analyzing the dynamic effects of permanent and transitory shocks. *Journal of Economic dynamics and Control*, *25*(10), 1527–1546.

Hafner, C. M., & Herwartz, H. (1998). Structural analysis of portfolio risk using beta impulse response functions. *Statistica Neerlandica*, *52*(3), 336–355.

Hafner, C. M., & Herwartz, H. (2006). Volatility impulse responses for multivariate GARCH models: An exchange rate illustration. *Journal of International Money and Finance*, *25*, 719–740.

Han, H., & Park, J. Y. (2012). Arch/garch with persistent covariate: Asymptotic theory of mle. *Journal of Econometrics*, *167*(1), 95–112.

Hasanov, A. S., Do, H. X., & Shaiban, M. S. (2016). Fossil fuel price uncertainty and feedstock edible oil prices: Evidence from MGARCH-M and VIRF analysis. *Energy Economics*, *57*, 16–27.

Hasanov, A. S., Poon, W. C., Alfreedi, A. A., & Heng, Z. Y. (2018). Forecasting volatility in the biofuel feedstock markets in the presence of structural breaks: A comparison of alternative distribution functions. *Energy Economics*, *70*, 307–333.

Hasbrouck, J. (1995). One security, many markets: Determining the contributions to price discovery. *The journal of Finance*, *50*(4), 1175–1199.

Hassouneh, I., Serra, T., Bojnec, Š., & Gil, J. (2017). Modelling price transmission and volatility spillover in the Slovenian wheat market. *Applied Economics*, *49*(41), 4116–4126.

Headey, D., & Fan, S. (2008). Anatomy of a crisis: The causes and consequences of surging food prices. *Agricultural economics*, *39*, 375–391.

Hochman, G., Rajagopal, D., Timilsina, G. R., & Zilberman, D. (2011). The role of inventory adjustments in quantifying factors causing food price inflation. *World Bank Policy Research Working Paper*, (5744).

Johansen, S. (1991). Estimation and hypothesis testing of cointegration vectors in gaussian vector autoregressive models. *Econometrica*, 1551–1580.

Kim, K., & Chavas, J.-P. (2002). A dynamic analysis of the effects of a price support program on price dynamics and price volatility. *Journal of Agricultural and Resource Economics*, 495–514.

Koop, G., Pesaran, M. H., & Potter, S. M. (1996). Impulse response analysis in nonlinear multivariate models. *Journal of econometrics*, *74*(1), 119–147.

Ljung, G. M., & Box, G. E. (1978). On a measure of lack of fit in time series models. *Biometrika*, *65*(2), 297–303.

Lütkepohl, H. (1997). *Handbook of matrices* (J. Wiley & Sons, Eds.). John Wiley; Sons.
Lütkepohl, H. (2005). *New introduction to multiple time series analysis*. Springer Science & Business Media.
Marchant, M. A., & Wang, H. H. (2018). Theme overview: Us–china trade dispute and potential impacts on agriculture. choices, quarter 2.
Meyers, W. H., & Meyer, S. D. (2008). *Causes and implications of the food price surge* (tech. rep.). Food and Agricultural Policy Research Institute (FAPRI).
Mitchell, D. (2008). A note on rising food prices. *World bank policy research working paper*, (4682).
Moschini, G., & Myers, R. J. (2001). Testing for constant hedge ratios in commodity markets: A multivariate GARCH approach. *Journal of Empirical Finance*, *9*, 589–603.
Moser, B. R. (2008). Influence of blending canola, palm, soybean, and sunflower oil methyl esters on fuel properties of biodiesel. *Energy & fuels*, *22*(6), 4301–4306.
Murty, K. G. (1983). *Linear programming*. Springer.
Myers, R. J., Johnson, S. R., Helmar, M., & Baumes, H. (2014). Long-run and short-run co-movements in energy prices and the prices of agricultural feedstocks for biofuel. *American Journal of Agricultural Economics*, *96*(4), 991–1008.
Ng, V., & Pirrong, S. C. (1994). Fundamentals and volatility: Storage, spreads, and the dynamics of metals prices. *Journal of Business*, 203–230.
Paris, A. (2018). On the link between oil and agricultural commodity prices: Do biofuels matter? *International Economics*, *155*, 48–60.
Pesaran, H. H., & Shin, Y. (1998). Generalized impulse response analysis in linear multivariate models. *Economics letters*, *58*(1), 17–29.
Prakash, A. et al. (2011). Why volatility matters. *Safeguarding food security in volatile global markets*, 3–26.
Putniņš, T. J. (2013). What do price discovery metrics really measure? *Journal of Empirical Finance*, *23*, 68–83.
Qiu, C., Colson, G., Escalante, C., & Wetzstein, M. (2012). Considering macroeconomic indicators in the food before fuel nexus. *Energy Economics*, *34*(6), 2021–2028.
Sanders, D. J., Balagtas, J. V., & Gruère, G. P. (2014). Revisiting the palm oil boom in South-East Asia: Fuel versus food demand drivers. *Applied Economics*, *46*, 127–138.
Schwarz, T. V., & Szakmary, A. C. (1994). Price discovery in petroleum markets: Arbitrage, cointegration, and the time interval of analysis. *The Journal of Futures Markets*, *14*(2), 147.
Serra, T., & Gil, J. (2013). Price volatility in food markets: Can stock building mitigate price fluctuations? *European Review of Agricultural Economics*, *40*(3), 507–528.
Serra, T., & Zilberman, D. (2013). Biofuel-related price transmission literature: A review. *Energy Economics*, *37*, 141–151.
Serra, T., Zilberman, D., & Gil, J. (2011). Price volatility in ethanol markets. *European review of agricultural economics*, *38*(2), 259–280.
Shively, G. E. (1996). Food price variability and economic reform: An arch approach for ghana. *American Journal of Agricultural Economics*, *78*(1), 126–136.
Silvennoinen, A., & Teräsvirta, T. (2009). Multivariate GARCH models. *Handbook of financial time series* (pp. 201–229). Springer.
Stigler, M., & Prakash, A. (2011). The role of low stocks in generating volatility and panic. *Safeguarding food security in volatile global markets*, 327–341.
Tse, Y. K. (2000). A test for constant correlations in a multivariate GARCH model. *Journal of econometrics*, *98*(1), 107–127.
USDA. (2021). *Oilseeds: World markets and trade* (tech. rep.). USDA.

Vollmer, T., Herwartz, H., & von Cramon-Taubadel, S. (2020). Measuring price discovery in the European wheat market using the partial cointegration approach. *European Review of Agricultural Economics*, *47*(3), 1173–1200.

Williams, J. C., Wright, B. D. et al. (2005). Storage and commodity markets. *Cambridge Books*.

Wright, B. D. (2011). The economics of grain price volatility. *Applied Economic Perspectives and Policy*, *33*(1), 32–58.

Yan, B., & Zivot, E. (2010). A structural analysis of price discovery measures. *Journal of Financial Markets*, *13*(1), 1–19.

Zhen, M., Rude, J., & Qiu, F. (2018). Price volatility spillovers in the western Canadian feed barley, US corn, and Alberta cattle markets. *Canadian Journal of Agricultural Economics*, *66*(2), 209–229.

Appendix

A Model selection

A.1 Descriptive statistics and stationarity tests

		LEVELS			DIFFERENCE		
		RSO	SBO	PMO	RSO	SBO	PMO
Monthly	Mean	6.850	6.814	6.626	0.0019	0.0018	0.0037
	Std	0.1834	0.1912	0.2313	0.0421	0.0404	0.0643
	Shapiro	0.891***	0.908***	0.980***	0.976**	0.985	0.992
	Jarque-Bera	19.0***	14.6***	3.19	11.8***	2.69	0.348
	ADF	−1.89	−1.82	−2.05	−8.33***	−7.29***	−7.77***
	PP	−1.62	−1.57	−2.06	−8.72***	−8.33***	−8.41***
	KPSS	1.70***	2.24***	2.15***	0.164	0.189	0.154
Daily	Mean	6.739	6.708	6.508	4.99E−05	9.59E−05	7.45E−05
	Std	0.0763	0.0975	0.1452	0.0122	0.0119	0.0179
	Shapiro	0.981***	0.982***	0.985***	0.928***	0.956***	0.959***
	Jarque−Bera	75.4***	54.7***	25.8***	2042***	1190***	612***
	ADF	−2.19	−1.63	−1.51	−34.5***	−31.6***	−26.6***
	PP	−2.53	−1.75	−1.72	−51.9***	−45.6***	−53.3***
	KPSS	5.32***	12.5***	8.52***	0.163	0.256	0.315

Table A1: **Descriptive statistics and unit-root tests**
Note: A constant is used as a deterministic component for unit-root tests. *, **, and *** indicate statistical significance at the 10%, 5%, and 1% levels, respectively.

	Monthly			Daily		
	None	Const	Trend	None	Const	Trend
$r = 0$	−1646.5	−1636.2	−1636.6	−31683.4	−31673.7	−31665.2
$r = 1$	**−1654.5**	−1649.5	−1651.3	**−31708.2**	−31703.2	−31703.1
$r = 2$	−1651.2	−1642.0	−1646.3	−31690.8	−31686.3	−31678.3
$r = 3$	−1626.8	−1612.5	−1612.2	−31642.9	−31620.5	−31622.0

Table A2: BIC values for different cointegration ranks and deterministic terms

	Monthly		Daily	
	Stat	p-value	Stat	p-value
$r = 0$	30.67***	0.007	29.90***	0.009
$r = 1$	11.78*	0.062	5.21	0.585
$r = 2$	0.23	0.755	0.08	0.813

Table A3: Johansen tests (no deterministic term)

A.2 Stepwise method

Table A4 shows the detailed results of the stepwise method to determine the optimal exogenous variables for each model. We first determine the optimal exogenous variables for the conditional mean, and we subsequently find those associated with the conditional volatility dynamics.

To determine the exogenous variables to add in each conditional mean and variance models, we consider the AIC criterion. We always select the model with the lowest criterion value: $\text{AIC} = 2k - 2L_T(\theta)$, with k the number of model parameters to estimate, and $L_T(\theta)$ the log-likelihood of our model. From equation (1), we see that if we add an exogenous variable to

the conditional mean model, we will need to estimate K $(= 3)$ additional parameters, and if we add an exogenous variable to the conditional variance model, we will need to estimate ${}^{K\times(K+1)}/_{2}$ $(= 6)$ additional parameters. It is therefore easy to see that the addition of an exogenous variable will be relevant if the log-likelihood of the model increases by at least 3 for an exogenous variable in the conditional mean model, and by at least 6 in the conditional variance model. We could also have used the likelihood ratio statistic to determine whether the addition of an exogenous variable is relevant, but this would have been more restrictive. Adding an exogenous variable would have been relevant if the log-likelihood of our model would have increased by 6.25 $(\chi^2_{10\%}(3))$ for the conditional mean model, or by 10.64 $(\chi^2_{10\%}(6) = 10.64)$ for the conditional variance model.

The stepwise method consists of independently trying all the exogenous variables one by one and then selecting the one with the lowest AIC value. We then combine this with the remaining exogenous variables and select the best marginal contributor. We repeat this operation until none of the exogenous variables improves our model, i.e., in our study, until none improves the AIC. Details of the log-likelihood values obtained at each step of the stepwise method are given in Table A4, and Table A5 summarises the results.

The tables have to be read row by row: for each row, we determine which exogenous variable is the best – that is to say, the variable that maximises the log-likelihood value when we add it to the model. Once we determine which exogenous variable is the best and check if it improves the model, we add it to the model and we can then go on to the next row. We keep iterating until the addition of any remaining exogenous variable does not improve our model according to the AIC criterion. The numbers of pre-iterations completed with the simplex algorithm is printed. In the monthly sample, we used the BHHH algorithm when the BFGS failed to converge, and 'NA' indicates that both the BHHH and BFGS algorithms failed to converge.

Table A6 and Table A7 show the estimated parameters for the determined optimal models, along with their associated statistical significances.

VECM

		LEVELS												DIFFERENCE									
Monthly	None	Brent	Tbills	Var Tbills	EURUSD	USDMYR	EURMYR	Ratio RSO	Ratio SBO	Ratio SFO	Ratio PMO	Ratio RS	Ratio SB	Brent	Tbills	EURUSD	USDMYR	EURMYR	Ratio RSO	Ratio SBO	Ratio SFO	Ratio PMO	Ratio RS	Ratio SB
0 exog	861.9	862.0	864.3	863.4	862.9	862.4	862.1	862.0	863.1	862.0	862.1	864.0	862.1	877.9	863.3	874.0	871.5	865.1	864.9	862.9	862.3	863.5	863.4	863.2
1 exog	-	878.0	881.3	879.3	879.2	878.5	878.2	878.0	879.1	878.1	878.2	880.0	878.3	X	878.3	884.7	882.7	881.0	881.2	879.2	878.3	879.7	879.5	878.9
2 exog	-	884.8	889.0	885.9	885.3	885.1	885.0	884.7	886.4	885.0	884.9	886.5	885.0	X	885.7	X	888.7	887.0	888.0	885.7	884.9	886.3	886.4	885.8
3 exog	-	889.3	X	889.4	889.5	889.4	889.8	890.3	889.7	889.0	890.6	891.5	889.4	X	889.4	X	893.6	891.8	891.9	889.6	890.2	890.5	890.4	889.6
4 exog	-	894.2	X	894.0	893.9	894.4	894.8	895.5	894.7	893.6	895.5	895.7	894.2	X	893.9	X	X	899.1	896.4	894.2	895.0	895.1	895.5	895.1
Daily	None	Brent	Tbills	Var Tbills	EURUSD	USDMYR	EURMYR	Ratio RSO	Ratio SBO	Ratio SFO	Ratio PMO	Ratio RS	Ratio SB	Brent	Tbills	EURUSD	USDMYR	EURMYR	Ratio RSO	Ratio SBO	Ratio SFO	Ratio PMO	Ratio RS	Ratio SB
0 exog	16 008.0	16 008.1	16 008.1	16 010.5	16 008.2	16 008.2	16 008.2	16 010.9	16 008.2	16 008.6	16 008.1	16 008.1	16 008.5	16 054.3	16 011.8	16 120.5	16 024.3	16 067.6	16 009.6	16 010.9	16 008.0	16 012.4	16 008.5	16 008.3
1 exog	-	16 120.9	16 120.9	16 122.9	16 121.1	16 120.7	16 120.9	16 123.2	16 120.8	16 121.2	16 120.7	16 121.3	16 120.8	16 166.0	16 125.5	X	16 135.0	16 134.0	16 122.1	16 124.0	16 120.5	16 125.0	16 121.0	16 120.9
2 exog	-	16 166.5	16 166.4	16 167.9	16 166.7	16 166.4	16 166.6	16 168.7	16 166.5	16 166.8	16 166.3	16 166.9	16 166.4	X	16 168.9	X	16 176.3	16 175.2	16 167.3	16 169.5	16 166.0	16 169.7	16 166.5	16 166.3
3 exog	-	16 176.7	16 176.6	16 178.2	16 177.0	16 176.7	16 176.9	16 179.1	16 176.8	16 177.1	16 176.6	16 177.2	16 176.7	X	16 179.1	X	X	16 178.3	16 177.5	16 179.8	16 176.3	16 179.8	16 176.8	16 176.6
4 exog	-	16 180.2	16 180.0	16 181.7	16 180.5	16 180.2	16 180.3	16 182.8	16 180.3	16 180.6	16 180.1	16 180.5	16 180.3	X	16 182.5	X	X	16 181.8	16 181.9	16 183.3	16 179.8	X	16 180.2	16 179.9
5 exog	-	16 183.9	16 183.7	16 185.3	16 184.1	16 183.8	16 183.8	16 186.3	16 183.9	16 184.2	16 183.7	16 184.1	16 183.8	X	16 186.1	X	X	16 185.5	16 186.2	X	16 183.4	X	16 183.7	16 183.6

MGARCH

		LEVELS												DIFFERENCE									
Monthly	None	Brent	Tbills	VM Tbills	EURUSD	USDMYR	EURMYR	Ratio RSO	Ratio SBO	Ratio SFO	Ratio PMO	Ratio RS	Ratio SB	Brent	Tbills	EURUSD	USDMYR	EURMYR	Ratio RSO	Ratio SBO	Ratio SFO	Ratio PMO	Ratio RS	Ratio SB
0 exog	919.7	925.1	926.2	927.7	920.2	926.8	928.6	923.7	925.8	928.3	925.7	923.6	927.3	926.9	926.3	924.4	921.9	925.7	0.0	924.8	927.4	932.6	926.9	925.5
(Iter simplex)	0	0	0	0	0	0	0	0	0	0	0	0	0	0	0	0	0	0	NA	0	0	0	0	0
1 exog	-	938.0	942.0	939.0	935.9	937.5	938.5	935.1	938.9	938.2	935.9	936.1	936.6	936.0	936.8	935.2	934.9	936.3	933.6	939.1	937.3	X	937.8	934.2
(Iter simplex)	-	0	0	0	0	0	0	0	0	0	0	0	0	0	0	0	0	0	0	0	0	X	0	0
2 exog	-	941.3	X	948.0	945.3	942.1	944.2	944.5	938.3	946.2	946.8	942.9	937.4	945.4	938.9	948.9	941.0	947.8	941.6	943.9	944.3	X	944.9	942.9
(Iter simplex)	-	BHHH 0	X	5	0	0	0	10	BHHH 5	15	0	0	BHHH 3	0	BHHH 1	BHHH 5	BHHH 15	0	0	BHHH 25	2	X	0	5
3 exog	-	949.1	X	0.0	949.2	945.9	949.8	0.0	949.8	949.6	952.9	951.5	950.4	952.9	954.4	X	951.5	948.6	949.5	0.0	950.4	X	952.6	951.3
(Iter simplex)	-	BHHH 6	X	NA	BHHH 25	40	15	NA	35	10	15	0	45	0	BHHH 5	X	0	0	0	NA	0	X	0	0
Daily	None	Brent	Tbills	VM Tbills	EURUSD	USDMYR	EURMYR	Ratio RSO	Ratio SBO	Ratio SFO	Ratio PMO	Ratio RS	Ratio SB	Brent	Tbills	EURUSD	USDMYR	EURMYR	Ratio RSO	Ratio SBO	Ratio SFO	Ratio PMO	Ratio RS	Ratio SB
0 exog	16 482.8	16 488.4	16 496.7	16 506.9	16 491.2	16 498.5	16 508.1	16 507.3	16 480.8	16 483.0	16 493.5	16 491.0	16 489.4	16 487.5	16 486.5	16 502.5	16 499.7	16 515.7	16 485.7	16 484.6	16 495.0	16 495.0	16 508.2	16 486.0
(Iter simplex)	5	5	0	0	5	0	0	0	0	0	0	0	0	0	5	0	0	0	0	0	0	0	0	0
1 exog	-	16 505.7	16 512.8	16 524.8	16 524.8	16 529.0	16 525.5	16 513.8	16 518.9	16 503.7	16 524.7	16 524.1	16 508.4	16 527.8	16 517.4	16 523.1	16 517.8	X	16 521.4	16 518.5	16 515.1	16 524.9	16 520.2	16 504.1
(Iter simplex)	-	0	0	0	0	X	0	0	0	0	0	0	0	0	0	0	0	X	0	0	0	0	0	0
2 exog	-	16 537.1	16 538.4	16 546.2	16 540.2	X	16 537.6	16 550.4	16 515.9	16 542.1	16 549.9	16 538.2	16 544.9	16 542.9	16 539.3	16 550.9	16 544.3	X	16 520.2	16 541.1	16 560.0	16 538.6	16 542.8	16 515.3
(Iter simplex)	-	0	0	0	0	X	0	0	0	0	0	0	0	0	5	0	0	X	0	0	0	0	0	0
3 exog	-	16 554.1	16 557.7	16 564.4	16 572.6	X	16 573.6	16 580.0	16 562.7	16 543.6	16 572.8	16 566.5	16 569.9	16 572.4	16 567.3	16 565.2	16 561.1	X	16 543.6	16 562.4	X	16 565.9	16 564.3	16 544.0
(Iter simplex)	-	0	0	0	0	X	0	0	0	0	0	5	0	0	15	0	0	X	0	0	X	0	0	0
4 exog	-	16 592.2	16 576.3	16 582.1	16 575.7	X	16 594.4	X	16 586.6	16 593.2	16 583.7	16 585.7	16 583.9	16 585.4	16 584.8	16 596.5	16 589.1	X	16 579.2	16 591.3	X	16 588.9	16 582.8	16 590.1
(Iter simplex)	-	0	0	0	0	X	0	X	0	0	0	0	0	0	0	0	0	X	0	0	X	0	0	0
5 exog	-	16 607.4	16 588.3	16 590.3	16 594.0	X	16 595.6	X	16 609.4	16 604.4	16 597.5	16 585.6	16 615.1	16 593.8	16 595.6	X	16 601.3	X	16 602.4	16 605.8	X	16 579.8	16 574.8	16 599.6
(Iter simplex)	-	0	0	0	0	X	0	X	0	0	0	0	0	0	15	X	0	X	0	0	X	0	5	0
6 exog	-	16 622.9	16 614.9	16 619.8	16 600.6	X	16 585.0	X	16 635.7	16 613.7	16 584.5	16 607.1	X	16 607.8	16 627.4	X	16 619.4	X	16 607.5	16 619.3	X	16 604.2	16 617.9	16 621.4
(Iter simplex)	-	0	0	0	0	X	0	X	0	0	0	0	X	0	0	X	5	X	0	0	X	0	0	0
7 exog	-	16 648.9	16 643.1	16 620.0	16 641.9	X	16 634.7	X	X	16 648.7	16 647.0	16 623.4	X	16 636.7	16 605.8	X	16 636.3	X	16 646.6	16 622.6	X	16 612.3	16 640.0	16 641.9
(Iter simplex)	-	0	0	0	0	X	0	X	X	5	0	0	X	0	0	X	0	X	0	0	X	0	0	0
8 exog	-	X	16 655.0	16 637.9	16 650.4	X	16 643.9	X	X	16 665.0	16 645.3	16 647.8	X	16 654.5	16 648.2	X	16 663.5	X	16 647.5	16 662.3	X	16 645.9	16 648.2	16 653.3
(Iter simplex)	-	X	0	0	0	X	0	X	X	0	0	0	X	0	5	X	0	X	0	0	X	0	5	0
9 exog	-	X	16 670.4	16 679.5	16 667.9	X	16 663.5	X	X	X	16 666.6	16 661.4	X	16 644.7	16 672.0	X	16 670.2	X	16 664.0	16 653.1	X	16 665.0	16 667.9	16 663.3
(Iter simplex)	-	X	0	0	0	X	0	X	X	X	0	0	X	0	0	X	0	X	0	0	X	5	0	0
10 exog	-	X	16 668.8	X	16 660.7	X	16 664.0	X	X	X	16 658.6	16 691.7	X	16 680.6	16 652.4	X	16 673.0	X	16 657.8	16 676.4	X	16 655.7	16 669.9	16 677.7
(Iter simplex)	-	X	0	X	0	X	0	X	X	X	0	5	X	0	0	X	0	X	0	5	X	0	0	5
11 exog		X	16 690.9	X	16 683.0	X	16 694.6	X	X	X	16 670.8	X	X	16 689.9	16 666.0	X	16 678.7	X	16 697.3	16 668.7	X	16 666.2	16 686.6	16 693.7
(Iter simplex)		X	0	X	0	X	0	X	X	X	0	X	X	0	0	X	0	X	5	10	X	0	0	0

Table A4: Stepwise method to determine optimal exogenous variables for VECM and MGARCH (log-likelihood)

		LEVELS											
		Brent	Tbills	Var Tbills	EURUSD	USDMYR	EURMYR	Ratio RSO	Ratio SBO	Ratio SFO	Ratio PMO	Ratio RS	Ratio SB
VECM	Monthly		X										
	Daily												
GARCH	Monthly		X										
	Daily	X		X		X		X	X	X		X	X

		DIFFERENCE											LOG-LIKELIHOOD	
		Brent	Tbills	EURUSD	USDMYR	EURMYR	Ratio RSO	Ratio SBO	Ratio SFO	Ratio PMO	Ratio RS	Ratio SB	Without exog.	Optimal models
VECM	Monthly	X		X	X								861.9	893.6
	Daily	X		X	X			X		X			16 008.0	16 183.3
GARCH	Monthly			X						X			919.7	948.9
	Daily			X		X			X				16 482.8	16 691.7

Table A5: Optimal exogenous variables and model log-likelihood values

$$\alpha = \begin{pmatrix} 0.007 \\ 0.083^{**} \\ 0.266^{***} \end{pmatrix}, \beta = \begin{pmatrix} 1 \\ -0.381^{***} \\ -0.635^{***} \end{pmatrix}, \Gamma_1 = \begin{pmatrix} 0.199 & 0.095 & -0.043 \\ 0.103 & 0.131 & 0.008 \\ -0.323 & 0.363 & 0.224^{**} \end{pmatrix}$$

$$A = \begin{pmatrix} 0.747^{***} & 0.226 & 0.781^{**} \\ -0.661^{***} & -0.322 & -1.393^{***} \\ 0.180 & 0.230^{**} & 0.562^{**} \end{pmatrix}, B = \begin{pmatrix} 0.336 & 0.180 & -0.717^{**} \\ 0.115 & -0.150 & 0.753^{*} \\ -0.082 & 0.046 & 0.073 \end{pmatrix}, D = \begin{pmatrix} 0.274 & -0.141 & 0.494 \\ 0.237 & 1.143^{***} & 0.409 \\ 0.000 & -0.185 & -0.123 \end{pmatrix}$$

C^V	LEVELS	DIFFERENCE		
	Tbills	Brent	EURUSD	USDMYR
RSO (P_1)	0.064	0.00256^{***}	0.251^{*}	-0.040
SBO (P_2)	-0.704	0.00216^{***}	0.271^{**}	-0.093^{*}
PMO (P_3)	-2.054^{***}	0.00332^{***}	-0.144	-0.200^{**}

C^G		LEVELS	DIFFERENCE	
	C_0	Tbills	EURUSD	Ratio PMO
Var RSO	0.025^{***}	0.030	0.213	-0.715^{***}
Var SBO	0.013^{***}	-0.455	-0.062	0.463^{*}
Var PMO	0.006	0.043	0.432^{*}	0.786
Cov RSO–SBO	0.026^{***}	-1.199^{***}	0.290^{*}	0.015
Cov RSO–PMO	0.032^{***}	-0.501	0.407	0.470
Cov SBO–PMO	0.012	0.193	0.229	0.061

Table A6: Estimated parameters – monthly
Note: *, **, and *** indicate statistical significance at the 10%, 5%, and 1% levels, respectively.

A.3 Residuals tests

We can represent the standardised residuals as $\zeta_t = \Sigma_{t|t-1}^{-1/2}\varepsilon_t$. We can also verify the adequacy of the model by performing multivariate Ljung–Box tests (Ljung & Box, 1978) and Lagrange multiplier (LM) tests (Tse, 2000). These test whether there is still any serial correlation between innovation or any ARCH effect – i.e., serial correlation between squared innovations – which leads to heteroscedasticity. We can apply these tests to the VECM residuals ε_t and compare the obtained values with those obtained with tests applied to the standardised residuals ζ_t. Table A8 indicates perfect removal of both serial correlation and ARCH effects for the standardised residuals ζ_t. Figure A1 shows the evolution of the conditional variance and covariance estimated by our models. There is strong heteroscedasticity, and the PMO variance is higher than the others in all samples.

$$\alpha = \begin{pmatrix} -0.0127^{***} \\ 0.0090^{**} \\ -0.0094^{*} \end{pmatrix}, \beta = \begin{pmatrix} 1 \\ -2.110^{***} \\ 1.139^{***} \end{pmatrix}, \Gamma_1 = \begin{pmatrix} -0.262^{***} & 0.104^{***} & 0.028^{*} \\ 0.059^{**} & -0.123^{***} & 0.050^{***} \\ 0.116^{***} & 0.162^{***} & -0.304^{***} \end{pmatrix}$$

$$\Gamma_2 = \begin{pmatrix} -0.094^{***} & 0.036 & 0.021 \\ 0.046^{*} & -0.071^{***} & 0.051^{***} \\ 0.079^{**} & 0.113^{***} & -0.143^{***} \end{pmatrix}, \Gamma_3 = \begin{pmatrix} -0.032 & 0.025 & 0.048^{***} \\ -0.002 & -0.088^{***} & 0.043^{**} \\ 0.014 & 0.061 & -0.018 \end{pmatrix}, \Gamma_4 = \begin{pmatrix} -0.057^{**} & 0.019 & 0.025 \\ 0.009 & -0.068^{***} & 0.006 \\ -0.008 & -0.001 & -0.038 \end{pmatrix}$$

$$A = \begin{pmatrix} 0.323^{***} & -0.078^{***} & 0.021 \\ -0.153^{***} & 0.04 & -0.076^{*} \\ -0.066^{***} & -0.022 & -0.03 \end{pmatrix}, B = \begin{pmatrix} 0.808^{***} & -0.194^{***} & -0.072^{***} \\ -0.51^{***} & -0.837^{***} & -0.543^{***} \\ 0.053^{***} & 0.113^{**} & 1.012^{***} \end{pmatrix}, D = \begin{pmatrix} 0.196^{***} & 0.112^{***} & 0.034 \\ -0.075 & -0.152^{*} & 0.02 \\ -0.002 & 0.091^{**} & 0.032 \end{pmatrix}$$

C^V	DIFFERENCE				
	Brent	EURUSD	USDMYR	Ratio SBO	Ratio PMO
RSO (P_1)	1.70E−04***	0.709***	−0.014	0.107	−0.0058
SBO (P_2)	2.74E−04***	0.129***	−0.042**	0.014	0.0590**
PMO (P_3)	1.98E−04***	0.195***	−0.108***	−0.258*	0.0487

C^G	C_0	LEVELS								DIFFERENCE		
		Brent	Var Tbills	USDMYR	Ratio RSO	Ratio SBO	Ratio SFO	Ratio RS	Ratio SB	EURUSD	EURMYR	Ratio SFO
Var RSO	−0.020***	−1.93E−06	1.666***	0.0038***	0.034***	0.043	−0.033***	−0.054***	0.028***	0.134**	0.028**	−0.084***
Var SBO	0.088***	−2.43E−05***	−1.153***	−0.0077***	−0.091***	−0.451***	0.068***	0.025	−0.043***	−0.259***	0.001	−0.153***
Var PMO	0.015	4.83E−06	0.074	−0.0013	−0.070***	−0.043	0.006	−0.049*	0.011	0.163*	−0.057**	0.025
Cov RSO–SBO	0.003	−5.71E−06	0.440	−0.0023**	0.053***	0.017	−0.073***	0.020*	0.029***	−0.227***	0.024*	0.088**
Cov RSO–PMO	0.014	−2.73E−06	0.343	−0.0024**	0.014	−0.063	−0.026**	0.002	0.008	−0.064	−0.007	−0.002
Cov SBO–PMO	0.052***	−2.63E−05***	−1.404***	−0.0052***	−0.034**	−0.318***	0.075***	0.064***	−0.024***	0.082	−0.050**	−0.096***

Table A7: Estimated parameters – daily
Note: *, **, and *** indicate statistical significance at the 10%, 5%, and 1% levels, respectively.

	Monthly		Daily	
	ε_t	ζ_t	ε_t	ζ_t
Ljung–Box (5)	52.5 [0.206]	48.0 [0.353]	12.4 [1.000]	32.4 [0.919]
Ljung–Box (8)	82.8 [0.181]	76.2 [0.346]	47.4 [0.989]	63.1 [0.763]
Ljung–Box (10)	98.0 [0.265]	89.2 [0.503]	64.8 [0.979]	79.0 [0.789]
Ljung–Box (12)	115. [0.307]	112. [0.367]	90.8 [0.884]	106. [0.548]
Arch-LM (5)	81.6 [0.001]	38.6 [0.737]	370. [0.000]	53.2 [0.188]
Arch-LM (10)	111. [0.070]	82.3 [0.706]	634. [0.000]	88.0 [0.539]

Table A8: Ljung–Box and ARCH-LM tests with different lags, and their associated p-values

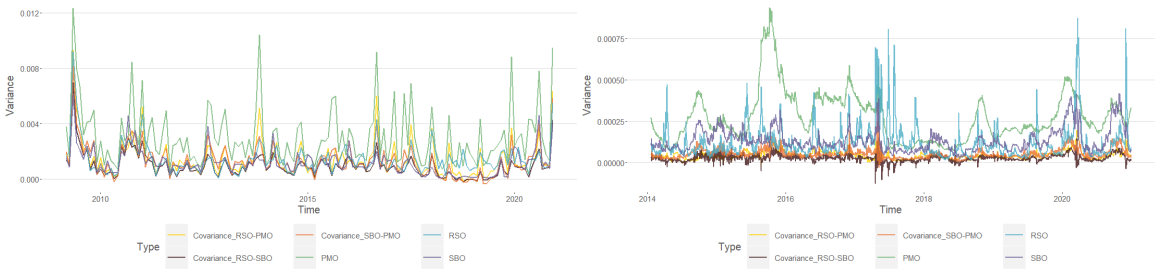

(a) Monthly. (b) Daily.

Figure A1: BEKK–GJR–MGARCH conditional variance.

B Covariance stationarity

The proof of covariance stationarity is derived from the work of Engle and Kroner (1995) and Lütkepohl (2005), to which we added both exogenous variables and an asymmetric term.

Using the properties

$$\begin{aligned}(\mathbf{A}\otimes\mathbf{B})^\tau &= \mathbf{A}^\tau\otimes\mathbf{B}^\tau\\ \operatorname{vec}(\mathbf{AXB}) &= (\mathbf{B}^\tau\otimes\mathbf{A})\operatorname{vec}(\mathbf{X})\\ \operatorname{vec}(\mathbf{A}+\mathbf{B}) &= \operatorname{vec}(\mathbf{A})+\operatorname{vec}(\mathbf{B})\end{aligned} \tag{10}$$

we can write our BEKK–MGARCH in the vec form:

$$\begin{aligned}\Sigma_{t|t-1} &= C_tC_t^\tau + A^\tau\varepsilon_{t-1}\varepsilon_{t-1}^\tau A + B^\tau\Sigma_{t-1|t-2}B + D^\tau\xi_{t-1}\xi_{t-1}^\tau D\\ \operatorname{vec}(\Sigma_{t|t-1}) &= \operatorname{vec}(C_tC_t^\tau + A^\tau\varepsilon_{t-1}\varepsilon_{t-1}^\tau A + B^\tau\Sigma_{t-1|t-2}B + D^\tau\xi_{t-1}\xi_{t-1}^\tau D)\\ &= \operatorname{vec}(C_tC_t^\tau) + \operatorname{vec}(A^\tau\varepsilon_{t-1}\varepsilon_{t-1}^\tau A)\\ &\quad + \operatorname{vec}(B^\tau\Sigma_{t-1|t-2}B) + \operatorname{vec}(D^\tau\xi_{t-1}\xi_{t-1}^\tau D)\\ &= (C_t\otimes C_t)\operatorname{vec}(\mathbf{I}) + (A\otimes A)^\tau\operatorname{vec}(\varepsilon_{t-1}\varepsilon_{t-1}^\tau)\\ &\quad + (B\otimes B)^\tau\operatorname{vec}(\Sigma_{t-1|t-2}) + (D\otimes D)^\tau\operatorname{vec}(\xi_{t-1}\xi_{t-1}^\tau)\\ &= C_t^{\text{vec}} + A^{\text{vec}}\operatorname{vec}(\varepsilon_{t-1}\varepsilon_{t-1}^\tau) + B^{\text{vec}}\operatorname{vec}(\Sigma_{t-1|t-2}) + D^{\text{vec}}\operatorname{vec}(\xi_{t-1}\xi_{t-1}^\tau)\end{aligned} \tag{11}$$

and note:

$$\begin{cases} C_t^{\text{vec}} &= (C_t\otimes C_t)\operatorname{vec}(\mathbf{I})\\ A^{\text{vec}} &= (A\otimes A)^\tau\\ B^{\text{vec}} &= (B\otimes B)^\tau\\ D^{\text{vec}} &= (D\otimes D)^\tau\end{cases} \tag{12}$$

Following Hafner and Herwartz (1998), and thanks to the symmetry of the distribution of ε_t, we can write:

$$\begin{aligned}E[\operatorname{vec}(\xi_t\xi_t^\tau)|\mathcal{F}_{t-1}] &= E\left[\operatorname{vec}\left((\varepsilon_t\circ\mathbb{1}_{x>0})(\varepsilon_t\circ\mathbb{1}_{x>0})^\tau\right)|\mathcal{F}_{t-1}\right]\\ &= \frac{1}{2}E[\operatorname{vec}(\varepsilon_t\varepsilon_t^\tau)|\mathcal{F}_{t-1}]\end{aligned} \tag{13}$$

We can then write the conditional expectations iteratively, knowing that $\Sigma_{t|t-1} = E[\varepsilon_t\varepsilon_t^\tau|\mathcal{F}_{t-1}]$. We thus obtain (see proof proposition 2.7 of Engle and Kroner (1995) for details):

$$\begin{aligned}\operatorname{vec}(\Sigma_{t|t-2}) &= C_{t|t-2}^{\text{vec}} + A^{\text{vec}}E[\operatorname{vec}(\varepsilon_{t-1}\varepsilon_{t-1}^\tau)|\mathcal{F}_{t-2}]\\ &\quad + B^{\text{vec}}E[\operatorname{vec}(\Sigma_{t-1|t-2})|\mathcal{F}_{t-2}] + D^{\text{vec}}E[\operatorname{vec}(\xi_{t-1}\xi_{t-1}^\tau)|\mathcal{F}_{t-2}]\\ &= C_{t|t-2}^{\text{vec}} + A^{\text{vec}}\operatorname{vec}(\Sigma_{t-1|t-2})\\ &\quad + B^{\text{vec}}\operatorname{vec}(\Sigma_{t-1|t-2}) + \frac{1}{2}D^{\text{vec}}\operatorname{vec}(\Sigma_{t-1|t-2})\\ &= C_{t|t-2}^{\text{vec}} + \left[A^{\text{vec}} + B^{\text{vec}} + \frac{1}{2}D^{\text{vec}}\right]\operatorname{vec}(\Sigma_{t-1|t-2})\end{aligned} \tag{14}$$

$$
\begin{aligned}
\operatorname{vec}(\Sigma_{t|t-3}) &= C^{\text{vec}}_{t|t-3} + A^{\text{vec}} E[\operatorname{vec}(\varepsilon_{t-1}\varepsilon^{\tau}_{t-1})|\mathcal{F}_{t-3}] \\
&\quad + B^{\text{vec}} \operatorname{vec}(\Sigma_{t-1|t-3}) + D^{\text{vec}} E[\operatorname{vec}(\xi_{t-1}\xi^{\tau}_{t-1})|\mathcal{F}_{t-3}] \\
&= C^{\text{vec}}_{t|t-3} + A^{\text{vec}} E[\operatorname{vec}(\varepsilon_{t-1}\varepsilon^{\tau}_{t-1})|\mathcal{F}_{t-3}] \\
&\quad + B^{\text{vec}} \{C^{\text{vec}}_{t-1|t-3} + A^{\text{vec}} E[\operatorname{vec}(\varepsilon_{t-2}\varepsilon^{\tau}_{t-2})|\mathcal{F}_{t-3}] \\
&\quad + B^{\text{vec}} \operatorname{vec}(\Sigma_{t-2|t-3}) + D^{\text{vec}} E[\operatorname{vec}(\xi_{t-2}\xi^{\tau}_{t-2})|\mathcal{F}_{t-3}]\} \\
&\quad + \frac{1}{2} D^{\text{vec}} E[\operatorname{vec}(\varepsilon_{t-1}\varepsilon^{\tau}_{t-1})|\mathcal{F}_{t-3}] \\
&= C^{\text{vec}}_{t|t-3} + B^{\text{vec}} C^{\text{vec}}_{t-1|t-3} + A^{\text{vec}} E[\operatorname{vec}(\varepsilon_{t-1}\varepsilon^{\tau}_{t-1})|\mathcal{F}_{t-3}] \\
&\quad + B^{\text{vec}} \{A^{\text{vec}} \operatorname{vec}(\Sigma_{t-2|t-3}) \\
&\quad + B^{\text{vec}} \operatorname{vec}(\Sigma_{t-2|t-3}) + \frac{1}{2} D^{\text{vec}} \operatorname{vec}(\Sigma_{t-2|t-3})\} \\
&\quad + \frac{1}{2} D^{\text{vec}} E[\operatorname{vec}(\varepsilon_{t-1}\varepsilon^{\tau}_{t-1})|\mathcal{F}_{t-3}] \\
&= C^{\text{vec}}_{t|t-3} + B^{\text{vec}} C^{\text{vec}}_{t-1|t-3} + A^{\text{vec}} E[\operatorname{vec}(\varepsilon_{t-1}\varepsilon^{\tau}_{t-1})|\mathcal{F}_{t-3}] \\
&\quad + B^{\text{vec}} \{A^{\text{vec}} + B^{\text{vec}} + \frac{1}{2} D^{\text{vec}}\} \operatorname{vec}(\Sigma_{t-2|t-3}) \\
&\quad + \frac{1}{2} D^{\text{vec}} E[\operatorname{vec}(\varepsilon_{t-1}\varepsilon^{\tau}_{t-1})|\mathcal{F}_{t-3}] \\
&= C^{\text{vec}}_{t|t-3} + \{B^{\text{vec}} + A^{\text{vec}} + \frac{1}{2} D^{\text{vec}}\} C^{\text{vec}}_{t-1|t-3} \\
&\quad + A^{\text{vec}} \{A^{\text{vec}} + B^{\text{vec}} + \frac{1}{2} D^{\text{vec}}\} \operatorname{vec}(\Sigma_{t-2|t-3}) \\
&\quad + B^{\text{vec}} \{A^{\text{vec}} + B^{\text{vec}} + \frac{1}{2} D^{\text{vec}}\} \operatorname{vec}(\Sigma_{t-2|t-3}) \\
&\quad + \frac{1}{2} D^{\text{vec}} \{A^{\text{vec}} + B^{\text{vec}} + \frac{1}{2} D^{\text{vec}}\} \operatorname{vec}(\Sigma_{t-2|t-3}) \\
&= C^{\text{vec}}_{t|t-3} + \{B^{\text{vec}} + A^{\text{vec}} + \frac{1}{2} D^{\text{vec}}\} C^{\text{vec}}_{t-1|t-3} \\
&\quad + \{A^{\text{vec}} + B^{\text{vec}} + \frac{1}{2} D^{\text{vec}}\}^2 \operatorname{vec}(\Sigma_{t-2|t-3})
\end{aligned} \tag{15}
$$

$$
\begin{aligned}
\operatorname{vec}(\Sigma_{t|t-s}) = &\sum_{k=0}^{s-2} \{A^{\text{vec}} + B^{\text{vec}} + \frac{1}{2} D^{\text{vec}}\}^k C^{\text{vec}}_{t-k|t-s} \\
&+ \{A^{\text{vec}} + B^{\text{vec}} + \frac{1}{2} D^{\text{vec}}\}^{s-1} \operatorname{vec}(\Sigma_{t-s+1|t-s})
\end{aligned} \tag{16}
$$

Furthermore, provided that:

$$
\lim_{s\to\infty} \mathbf{X}^s = 0 \Leftrightarrow \text{ Spectral radius of } \mathbf{X} \text{ is less than 1,} \tag{17}
$$

it is necessary and sufficient for the limit $\lim_{s\to\infty} \operatorname{vec}(\Sigma_{t|t-s})$ to both exist and be finite for all the moduli of the eigenvalues associated with the matrix $\{A^{\text{vec}} + B^{\text{vec}} + \frac{1}{2} D^{\text{vec}}\}$ to be less than one. This is therefore the necessary and sufficient condition for MGARCH stationarity.

C MGARCH p-value derivation

The derivation of the conditional variance equation leads to a product, or even a sum of products, of estimated parameters. Therefore, we need to estimate the p-values associated with these parameter combinations. Let $X = (x_1, \cdots, x_N)$ be an $(N \times 1)$ vector of estimators, with N an even number. We note that $\hat{X}$ are the estimated parameters for X. We can then define the function f as:

$$f(X) = \sum_{i=1}^{N/2} x_{2(i-1)+1} x_{2i} = x_1 x_2 + x_3 x_4 + \cdots + x_{N-1} x_N \tag{18}$$

In equation (1), it is easy to see that we can express parameter combinations with this function f. We can approximate $f(X)$ with a first-order Taylor development around $\hat{X}$:

$$\begin{aligned} f(X) &\approx f(\hat{X}) \; + \; \sum_{i=1}^{N} \frac{\partial f(X)}{\partial x_i}\Big|_{\{\hat{X}\}} (X - \hat{X}) \\ &\approx f(\hat{X}) \; - \; \sum_{i=1}^{N} \frac{\partial f(X)}{\partial x_i}\Big|_{\{\hat{X}\}} \hat{X} \; + \; \sum_{i=1}^{N} \frac{\partial f(X)}{\partial x_i}\Big|_{\{\hat{X}\}} X \end{aligned} \tag{19}$$

We can now calculate the variance of this function of estimators, and we note that only the last element has a variance: the two other elements are fixed numbers.

$$\mathrm{Var}(f(X)) \approx \mathrm{Var}\left(\sum_{i=1}^{N} \frac{\partial f(X)}{\partial x_i}\Big|_{\{\hat{X}\}} X \right), \qquad \text{with: } \frac{\partial f(X)}{\partial x_i} = \begin{cases} x_{i-1} & \text{if } i \text{ is even} \\ x_{i+1} & \text{otherwise} \end{cases} \tag{20}$$

We then obtain the variance of $f(X)$ using the standard variance formula for the sum of N variables:

$$\mathrm{Var}(f(X)) \approx \sum_{i=1}^{N} \left(\frac{\partial f(X)}{\partial x_i}\Big|_{\{\hat{X}\}} \right)^2 \mathrm{Var}\left(x_i\right) \; + \; 2 \sum_{1 \le i < j \le N} \left(\frac{\partial f(X)}{\partial x_i}\Big|_{\{\hat{X}\}} \right) \left(\frac{\partial f(X)}{\partial x_j}\Big|_{\{\hat{X}\}} \right) \mathrm{Cov}(x_i, x_j) \tag{21}$$

We obtain all $\mathrm{Var}(x_i)$ and $\mathrm{Cov}(x_i, x_j)$ thanks to the Hessian matrix, and we then calculate the standard errors associated with each estimated parameter combination of our MGARCH model. We finally easily obtain the p-values associated with these parameter combinations.

In the following, we detail the parameter combinations for each variable of equation (1), along with their associated standard errors, for $(\Sigma_{t|t-1})_{i,j}$.

• Estimated parameter combinations:

$$\begin{aligned} \varepsilon_{k,t-1}\varepsilon_{l,t-1} &\longrightarrow A_{ki}A_{lj} + \mathbb{1}_{x \neq 0}(k-l) A_{li}A_{kj} \\ (\Sigma_{t-1|t-2})_{k,l} &\longrightarrow B_{ki}B_{lj} + \mathbb{1}_{x \neq 0}(k-l) B_{li}B_{kj} \\ \xi_{k,t-1}\xi_{l,t-1} &\longrightarrow D_{ki}D_{lj} + \mathbb{1}_{x \neq 0}(k-l) D_{li}D_{kj} \\ z_{l,t}z_{m,t} &\longrightarrow \sum_{k=1}^{\min(i,j)} (C_{z_l}^G)_{ik}(C_{z_m}^G)_{jk} + \mathbb{1}_{x \neq 0}(l-m)(C_{z_m}^G)_{ik}(C_{z_l}^G)_{jk} \end{aligned} \tag{22}$$

• Associated standard errors:

$$
\begin{aligned}
\varepsilon_{k,t-1}\varepsilon_{l,t-1} \longrightarrow\ & A_{lj}^2 \operatorname{Var}(A_{ki}) + A_{ki}^2 \operatorname{Var}(A_{lj}) + 2A_{lj}A_{ki} \operatorname{Cov}(A_{ki}A_{lj}) \\
& + \mathbb{1}_{x\neq 0}(k-l)\{A_{kj}^2 \operatorname{Var}(A_{li}) + A_{li}^2 \operatorname{Var}(A_{kj}) \\
& + 2[A_{lj}A_{kj} \operatorname{Cov}(A_{ki}A_{li}) + A_{lj}A_{li} \operatorname{Cov}(A_{ki}A_{kj}) \\
& + A_{ki}A_{kj} \operatorname{Cov}(A_{lj}A_{li}) + A_{ki}A_{li} \operatorname{Cov}(A_{lj}A_{kj}) + A_{kj}A_{li} \operatorname{Cov}(A_{li}A_{kj})]\} \\
(\Sigma_{t-1|t-2})_{k,l} \longrightarrow\ & B_{lj}^2 \operatorname{Var}(B_{ki}) + B_{ki}^2 \operatorname{Var}(B_{lj}) + 2B_{lj}B_{ki} \operatorname{Cov}(B_{ki}B_{lj}) \\
& + \mathbb{1}_{x\neq 0}(k-l)\{B_{kj}^2 \operatorname{Var}(B_{li}) + B_{li}^2 \operatorname{Var}(B_{kj}) \\
& + 2[B_{lj}B_{kj} \operatorname{Cov}(B_{ki}B_{li}) + B_{lj}B_{li} \operatorname{Cov}(B_{ki}B_{kj}) \\
& + B_{ki}B_{kj} \operatorname{Cov}(B_{lj}B_{li}) + B_{ki}B_{li} \operatorname{Cov}(B_{lj}B_{kj}) + B_{kj}B_{li} \operatorname{Cov}(B_{li}B_{kj})]\} \\
\xi_{k,t-1}\xi_{l,t-1} \longrightarrow\ & D_{lj}^2 \operatorname{Var}(D_{ki}) + D_{ki}^2 \operatorname{Var}(D_{lj}) + 2D_{lj}D_{ki} \operatorname{Cov}(D_{ki}D_{lj}) \\
& + \mathbb{1}_{x\neq 0}(k-l)\{D_{kj}^2 \operatorname{Var}(D_{li}) + D_{li}^2 \operatorname{Var}(D_{kj}) \\
& + 2[D_{lj}D_{kj} \operatorname{Cov}(D_{ki}D_{li}) + D_{lj}D_{li} \operatorname{Cov}(D_{ki}D_{kj}) \\
& + D_{ki}D_{kj} \operatorname{Cov}(D_{lj}D_{li}) + D_{ki}D_{li} \operatorname{Cov}(D_{lj}D_{kj}) + D_{kj}D_{li} \operatorname{Cov}(D_{li}D_{kj})]\} \\
z_{l,t}^2 \longrightarrow\ & \sum_{k,s=1}^{\min(i,j)} \operatorname{Cov}\left[(C_{z_l}^G)_{ik}, (C_{z_l}^G)_{is}\right] (C_{z_l}^G)_{jk}(C_{z_l}^G)_{js} \\
& + \operatorname{Cov}\left[(C_{z_l}^G)_{jk}, (C_{z_l}^G)_{js}\right] (C_{z_l}^G)_{ik}(C_{z_l}^G)_{is} + 2\operatorname{Cov}\left[(C_{z_l}^G)_{ik}, (C_{z_l}^G)_{js}\right] (C_{z_l}^G)_{jk}(C_{z_l}^G)_{is} \\
z_{l,t}z_{m,t} \underset{(l\neq m, i=j)}{\longrightarrow}\ & 4\sum_{k,s=1}^{i} \operatorname{Cov}\left[(C_{z_l}^G)_{ik}, (C_{z_l}^G)_{is}\right] (C_{z_m}^G)_{ik}(C_{z_m}^G)_{is} \\
& + \operatorname{Cov}\left[(C_{z_m}^G)_{ik}, (C_{z_m}^G)_{is}\right] (C_{z_l}^G)_{ik}(C_{z_l}^G)_{is} + 2\operatorname{Cov}\left[(C_{z_l}^G)_{ik}, (C_{z_m}^G)_{is}\right] (C_{z_m}^G)_{ik}(C_{z_l}^G)_{is} \\
z_{l,t}z_{m,t} \underset{(l\neq m, i\neq j)}{\longrightarrow}\ & \sum_{\substack{x_1,x_2\in\{i,j\} \\ y_1,y_2\in\{i,j\} \\ x_1\neq x_2, y_1\neq y_2}} \sum_{\substack{v_1,v_2\in\{l,m\} \\ w_1,w_2\in\{l,m\} \\ v_1\neq v_2, w_1\neq w_2}} \sum_{k,s=1}^{\min(i,j)} \left\{\operatorname{Cov}\left[(C_{z_{v_1}}^G)_{x_1k}, (C_{z_{w_1}}^G)_{y_1s}\right] (C_{z_{v_2}}^G)_{x_2k}(C_{z_{w_2}}^G)_{y_2s}\right\}
\end{aligned}
\tag{23}
$$

If we focus on variances, that is to say $(\Sigma_{t|t-1})_{i,j}$ with $i = j$, the standard error expressions are greatly simplified:

$$
\begin{aligned}
\varepsilon_{k,t-1}\varepsilon_{l,t-1} &\longrightarrow (1 + 3\mathbb{1}_{x\neq 0}(k-l))\left[A_{li}^2 \operatorname{Var}(A_{ki}) + A_{ki}^2 \operatorname{Var}(A_{li}) + 2A_{li}A_{ki} \operatorname{Cov}(A_{ki}A_{li})\right] \\
(\Sigma_{t-1|t-2})_{k,l} &\longrightarrow (1 + 3\mathbb{1}_{x\neq 0}(k-l))\left[B_{li}^2 \operatorname{Var}(B_{ki}) + B_{ki}^2 \operatorname{Var}(B_{li}) + 2B_{li}B_{ki} \operatorname{Cov}(B_{ki}B_{li})\right] \\
\xi_{k,t-1}\xi_{l,t-1} &\longrightarrow (1 + 3\mathbb{1}_{x\neq 0}(k-l))\left[D_{li}^2 \operatorname{Var}(D_{ki}) + D_{ki}^2 \operatorname{Var}(D_{li}) + 2D_{li}D_{ki} \operatorname{Cov}(D_{ki}D_{li})\right] \\
z_{l,t}^2 &\longrightarrow 4\sum_{k,s=1}^{i} \operatorname{Cov}\left[(C_{z_l}^G)_{ik}, (C_{z_l}^G)_{is}\right] (C_{z_l}^G)_{ik}(C_{z_l}^G)_{is}
\end{aligned}
\tag{24}
$$

$(\Sigma_{t\|t-1})_{11}$	1	z_1	z_2	z_3	z_4	z_5	z_6	z_7	z_8	z_9	z_{10}	z_{11}
1	4.16E−04											
z_1	7.87E−08	3.72E−12										
z_2	−6.80E−02**	−6.42E−06	2.78E00**									
z_3	−1.54E−04*	−1.46E−08	1.26E−02***	1.43E−05*								
z_4	−1.39E−03**	−1.31E−07	1.13E−01***	2.58E−04***	1.16E−03**							
z_5	−1.75E−03	−1.65E−07	1.43E−01	3.24E−04	2.92E−03	1.83E−03						
z_6	1.35E−03**	1.28E−07	−1.10E−01**	−2.50E−04**	−2.26E−03**	−2.84E−03	1.10E−03*					
z_7	2.20E−03***	2.08E−07	−1.80E−01**	−4.08E−04***	−3.67E−03**	−4.62E−03	3.57E−03**	2.91E−03				
z_8	−1.15E−03***	−1.08E−07	9.37E−02***	2.13E−04***	1.92E−03**	2.41E−03	−1.86E−03***	−3.03E−03*	7.91E−04*			
z_9	−5.46E−03*	−5.16E−07	4.46E−01**	1.01E−03*	9.11E−03*	1.15E−02	−8.85E−03*	−1.44E−02*	7.52E−03*	1.79E−02		
z_{10}	−1.15E−03**	−1.09E−07	9.42E−02**	2.14E−04**	1.93E−03**	2.42E−03	−1.87E−03**	−3.05E−03*	1.59E−03*	7.56E−03***	8.00E−04	
z_{11}	3.43E−03***	3.24E−07	−2.80E−01***	−6.37E−04***	−5.73E−03***	−7.21E−03	5.57E−03***	9.08E−03***	−4.73E−03***	−2.25E−02**	−4.76E−03*	7.08E−03**

$(\Sigma_{t\|t-1})_{22}$	1	z_1	z_2	z_3	z_4	z_5	z_6	z_7	z_8	z_9	z_{10}	z_{11}
1	7.75E−03***											
z_1	−4.31E−06***	6.22E−10***										
z_2	−2.00E−01***	5.10E−05***	1.52E00**									
z_3	−1.37E−03***	4.00E−07***	1.57E−02***	6.48E−05***								
z_4	−1.56E−02***	3.80E−06***	2.56E−01***	1.15E−03***	1.11E−02***							
z_5	−7.93E−02***	2.17E−05***	1.06E00***	6.87E−03***	8.38E−02***	2.04E−01***						
z_6	1.15E−02***	−2.47E−06**	−2.22E−01***	−7.08E−04**	−2.02E−02***	−6.40E−02***	1.00E−02***					
z_7	4.58E−03	−1.45E−06	−4.07E−02	−4.82E−04	−2.45E−03	−2.21E−02	5.02E−04	1.04E−03				
z_8	−7.33E−03***	1.75E−06***	1.24E−01***	5.24E−04**	1.09E−02***	3.96E−02***	−1.01E−02***	−9.99E−04	2.68E−03**			
z_9	−4.72E−02***	1.52E−05***	3.99E−01	5.05E−03***	2.29E−02	2.26E−01**	−2.02E−03	−2.22E−02*	9.01E−03	1.19E−01**		
z_{10}	3.39E−04	−3.23E−07	1.90E−02	−1.28E−04	2.39E−03	−5.16E−05	−3.41E−03	1.02E−03	1.32E−03	−1.15E−02	5.85E−04	
z_{11}	−2.64E−02***	6.43E−06***	4.31E−01***	1.95E−03***	3.72E−02***	1.41E−01***	−3.38E−02***	−4.21E−03	1.83E−02***	3.94E−02	3.97E−03	3.13E−02***

$(\Sigma_{t\|t-1})_{33}$	1	z_1	z_2	z_3	z_4	z_5	z_6	z_7	z_8	z_9	z_{10}	z_{11}
1	3.12E−03***											
z_1	−2.66E−06***	7.20E−10***										
z_2	−1.34E−01***	7.26E−05***	2.10E00**									
z_3	−6.44E−04***	2.71E−07***	1.26E−02**	3.43E−05***								
z_4	−5.15E−03***	1.01E−06	9.35E−02	4.61E−04**	6.19E−03***							
z_5	−3.61E−02***	1.66E−05***	8.45E−01***	3.70E−03***	2.56E−02***	1.07E−01***						
z_6	7.25E−03***	−3.76E−06***	−2.28E−01***	−6.64E−04***	−6.57E−03**	−4.51E−02***	6.37E−03***					
z_7	5.30E−03***	−3.86E−06***	−1.86E−01**	−5.46E−04***	2.57E−03	−3.70E−02***	9.02E−03**	6.53E−03**				
z_8	−2.01E−03*	1.35E−06***	7.58E−02**	1.86E−04*	3.77E−04	1.37E−02**	−3.98E−03**	−4.16E−03**	7.75E−04*			
z_9	1.15E−02	−2.39E−06	−2.51E−01	−9.60E−04	−3.00E−02**	−5.81E−02	1.75E−02	−5.65E−03	−1.57E−03	3.74E−02		
z_{10}	−7.10E−03***	2.13E−06	1.28E−01	7.01E−04**	1.11E−02***	3.77E−02**	−7.85E−03*	−9.36E−04	1.14E−03	−2.59E−02	5.80E−03**	
z_{11}	−9.32E−03***	5.31E−06***	2.73E−01***	9.37E−04***	2.86E−03	5.94E−02***	−1.41E−02***	−1.49E−02***	5.22E−03**	−7.28E−03	6.83E−03	9.92E−03**

$(\Sigma_{t\|t-1})_{21}$	1	z_1	z_2	z_3	z_4	z_5	z_6	z_7	z_8	z_9	z_{10}	z_{11}
1	−7.02E−05											
z_1	1.10E−07*	1.10E−11										
z_2	−3.24E−03	−1.04E−05	7.32E−01									
z_3	6.05E−05	−1.71E−08	−2.22E−03	−8.81E−06**								
z_4	−9.69E−04	−2.97E−07	1.04E−01***	1.22E−04	1.81E−03***							
z_5	−2.05E−04	−2.78E−07	4.76E−02	−3.44E−05	2.87E−03	7.39E−04						
z_6	1.38E−03	3.30E−07	−1.37E−01***	−2.01E−04*	−4.26E−03***	−3.71E−03	2.43E−03**					
z_7	−5.94E−04	2.69E−07	9.64E−03	2.01E−04**	−2.19E−03**	−7.32E−05	3.30E−03**	−1.08E−03				
z_8	−4.96E−04	−2.17E−07	6.08E−02***	4.44E−05	2.49E−03***	1.73E−03	−3.03E−03***	−1.00E−03	8.17E−04***			
z_9	5.09E−03***	−3.26E−07	−3.19E−01*	−1.17E−03***	−6.06E−04	−7.41E−03	−2.30E−03	1.49E−02**	−2.49E−03	−3.03E−02**		
z_{10}	−3.96E−04	−2.08E−07	5.27E−02*	2.56E−05	2.33E−03**	1.52E−03	−2.87E−03***	−7.37E−04	1.50E−03**	−3.18E−03	6.83E−04	
z_{11}	−2.09E−03**	3.10E−07	1.10E−01	5.30E−04***	−1.47E−03	2.33E−03	3.25E−03	−6.45E−03***	3.93E−05	3.09E−02***	4.64E−04	−7.43E−03***

$(\Sigma_{t\|t-1})_{31}$	1	z_1	z_2	z_3	z_4	z_5	z_6	z_7	z_8	z_9	z_{10}	z_{11}
1	−2.91E−04*											
z_1	2.83E−08	5.27E−12										
z_2	1.67E−02	−5.21E−06	5.71E−01									
z_3	1.04E−04**	−5.63E−09	−2.77E−03	−9.24E−06**								
z_4	1.99E−04	−1.20E−07	3.51E−02	−3.01E−05	4.78E−04							
z_5	1.89E−03	3.62E−09	−8.96E−02	−3.41E−04	−1.53E−03	−2.68E−03						
z_6	5.85E−05	1.41E−07	−5.47E−02*	−1.75E−05	−1.35E−03*	9.58E−04	8.60E−04					
z_7	−8.14E−04	1.43E−07	−1.48E−02	1.40E−04	−6.81E−04	3.47E−03	1.33E−03	−1.21E−04				
z_8	2.40E−04	−9.21E−08	2.28E−02	−3.89E−05	6.64E−04	−1.42E−03	−9.92E−04*	−3.62E−04	2.22E−04			
z_9	3.22E−03	−2.41E−07	−6.13E−02	−5.70E−04*	−3.12E−04	−1.11E−02	−1.35E−03	3.77E−03	−7.55E−04	−8.60E−03		
z_{10}	5.42E−04	−6.41E−08	−1.70E−03	−9.49E−05	1.64E−04	−2.06E−03	−5.09E−04	4.32E−04	3.05E−05	−2.73E−03*	−1.93E−04	
z_{11}	−1.15E−03	2.34E−07	−3.24E−02	1.97E−04	−1.25E−03	5.17E−03	2.26E−03**	−7.25E−05	−7.24E−04	5.12E−03	5.14E−04	1.81E−04

$(\Sigma_{t\|t-1})_{32}$	1	z_1	z_2	z_3	z_4	z_5	z_6	z_7	z_8	z_9	z_{10}	z_{11}
1	4.62E−03***											
z_1	−3.66E−06***	6.53E−10***										
z_2	−1.76E−01***	6.12E−05***	1.77E00***									
z_3	−8.96E−04***	3.48E−07***	1.49E−02***	4.54E−05***								
z_4	−6.86E−03***	2.97E−06***	1.91E−01***	5.64E−04**	3.79E−03**							
z_5	−5.14E−02***	1.99E−05***	9.79E−01***	4.88E−03***	4.10E−02***	1.43E−01***						
z_6	9.03E−03***	−3.27E−06***	−2.19E−01***	−6.91E−04***	−1.15E−02***	−5.15E−02***	7.03E−03***					
z_7	7.26E−03***	−2.29E−06***	−1.02E−01**	−6.80E−04***	−6.28E−03***	−3.83E−02***	5.59E−03**	1.67E−03				
z_8	−3.94E−03***	1.59E−06***	1.02E−01***	3.20E−04***	4.49E−03***	2.30E−02***	−6.22E−03***	−3.15E−03*	1.28E−03*			
z_9	−9.69E−03	5.80E−06	1.63E−01	1.41E−03	−5.37E−03	5.85E−02	−3.30E−03	−1.64E−02	−8.29E−04	−6.73E−03		
z_{10}	−4.05E−03	1.17E−06	6.19E−02	3.39E−04	4.51E−03	2.08E−02	−3.48E−03	−1.29E−03	2.12E−03	1.31E−02	−2.15E−04	
z_{11}	−1.52E−02***	6.13E−06***	3.56E−01***	1.32E−03***	1.50E−02***	8.67E−02***	−2.02E−02***	−1.21E−02**	8.51E−03***	7.17E−03	6.96E−03	1.46E−02***

Table C1: Conditional variance equations, exogenous variables (daily)
Note: z_1 = Brent, z_2 = VarTbills, z_3 = USDMYR, z_4 = RSO ratio, z_5 = SBO ratio, z_6 = SFO ratio, z_7 = RS ratio, z_8 = SB ratio, z_9 = ΔEURUSD, z_{10} = ΔEURMYR, z_{11} = ΔSFO ratio. *, **, and *** indicate statistical significance at the 10%, 5%, and 1% levels, respectively.

D VIRF of Hafner and Herwartz

Hafner and Herwartz (2006) developed the VIRF to study the impact and the persistence of a price shock on the volatility dependence structure with the MGARCH model. They defined the VIRF as the difference between the expected conditional variance–covariance matrix given an initial shock and state, and the expectation given the history is:

$$V_h(\zeta_t, \mathcal{F}_{t-1}) = E[\text{vech}(\Sigma_{t+h|t+h-1})|\mathcal{F}_{t-1}, \zeta_t] - E[\text{vech}(\Sigma_{t+h|t+h-1})|\mathcal{F}_{t-1}] \tag{25}$$

where ζ_t is the initial shock and $\mathcal{F}_{t-1}$ is all the information available on the market at time $t-1$. Following Appendix B and knowing that $\Sigma_{t|t-1}$ is symmetric as a variance–covariance matrix, we can easily rewrite our BEKK–MGARCH into its vech form, with D_K the duplication matrix, and D_K^+ its Moore–Penrose inverse:

$$\begin{cases} A^{\text{vech}} & = D_K^+ A^{\text{vec}} D_K = D_K^+ (A \otimes A)^\tau D_K \\ B^{\text{vech}} & = D_K^+ B^{\text{vec}} D_K = D_K^+ (B \otimes B)^\tau D_K \\ D^{\text{vech}} & = D_K^+ D^{\text{vec}} D_K = D_K^+ (D \otimes D)^\tau D_K \\ \text{vech}(\Sigma_{t|t-1}) & = D_K^+ \,\text{vec}(\Sigma_{t|t-1}) = \text{vech}(C_t^G C_t^{G\tau}) + A^{\text{vech}} \,\text{vech}(\varepsilon_{t-1}\varepsilon_{t-1}^\tau) \\ & \quad + B^{\text{vech}} \,\text{vech}(\Sigma_{t-1|t-2}) + D^{\text{vech}} \,\text{vech}(\xi_{t-1}\xi_{t-1}^\tau) \end{cases} \tag{26}$$

Hafner and Herwartz (2006) gave the analytical expression of the VIRF for MGARCH, but without asymmetry. To our knowledge, no previous study has developed the VIRF with asymmetry in analytical form. Provided that:

$$\begin{cases} (\mathbf{A} \circ \mathbf{B})^\tau & = \mathbf{A}^\tau \circ \mathbf{B}^\tau \\ \text{vec}(\mathbf{ABC}) & = (\mathbf{A} \otimes \mathbf{C}^\tau)\,\text{vec}(\mathbf{B}) \\ \mathbf{a} \circ \mathbf{b} & = \text{diag}(\mathbf{a})\mathbf{b} = \text{diag}(\mathbf{b})\mathbf{a} \qquad \text{(Hadamard product of two vectors)} \end{cases} \tag{27}$$

where diag is an operator that transforms a $K \times 1$ vector into a diagonal $(K \times K)$ square matrix, the diagonal of this matrix being the vector considered. We can then write:

$$\begin{aligned} \text{vec}(\xi_t\xi_t^\tau) &= \text{vec}\left\{[\varepsilon_t \circ \mathbb{1}_{x>0}(\varepsilon_t)]\,[\varepsilon_t \circ \mathbb{1}_{x>0}(\varepsilon_t)]^\tau\right\} \\ &= \text{vec}\left[\text{diag}\left\{\mathbb{1}_{x>0}(\varepsilon_t)\right\}\varepsilon_t\varepsilon_t^\tau\,\text{diag}\left\{\mathbb{1}_{x>0}(\varepsilon_t)\right\}\right] \\ &= \left[\text{diag}\left\{\mathbb{1}_{x>0}(\varepsilon_t)\right\} \otimes \text{diag}\left\{\mathbb{1}_{x>0}(\varepsilon_t)\right\}\right]\text{vec}(\varepsilon_t\varepsilon_t^\tau) \end{aligned} \tag{28}$$

Following Hafner and Herwartz (2006), we need to replace the residuals ε_t with the standardised residuals ζ_t. As $(\mathbf{A} \otimes \mathbf{B})(\mathbf{C} \otimes \mathbf{D}) = \mathbf{AC} \otimes \mathbf{BD}$, we can then write:

$$\begin{aligned} \text{vec}(\varepsilon_t\varepsilon_t^\tau) &= \text{vec}(\Sigma_{t|t-1}^{1/2}\zeta_t\zeta_t^\tau\Sigma_{t|t-1}^{1/2}) = \left[\Sigma_{t|t-1}^{1/2} \otimes \Sigma_{t|t-1}^{1/2}\right]\text{vec}(\zeta_t\zeta_t^\tau) \\ \text{vec}(\xi_t\xi_t^\tau) &= \left[\,\text{diag}\left\{\mathbb{1}_{x>0}(\Sigma_{t|t-1}^{1/2}\zeta_t)\right\} \otimes \text{diag}\left\{\mathbb{1}_{x>0}(\Sigma_{t|t-1}^{1/2}\zeta_t)\right\}\right]\left[\Sigma_{t|t-1}^{1/2} \otimes \Sigma_{t|t-1}^{1/2}\right]\text{vec}(\zeta_t\zeta_t^\tau) \\ &= \left[\left[\text{diag}\left\{\mathbb{1}_{x>0}(\Sigma_{t|t-1}^{1/2}\zeta_t)\right\}\Sigma_{t|t-1}^{1/2}\right] \otimes \left[\text{diag}\left\{\mathbb{1}_{x>0}(\Sigma_{t|t-1}^{1/2}\zeta_t)\right\}\Sigma_{t|t-1}^{1/2}\right]\right]\text{vec}(\zeta_t\zeta_t^\tau) \end{aligned} \tag{29}$$

Following Lütkepohl (2005), we retain $\Sigma_{t+h|t}$ as a convenient estimator for $E[\varepsilon_{t+h}\varepsilon_{t+h}^\tau|\mathcal{F}_t]$ with $h > 1$. Furthermore, knowing that $E[\xi_{t+h}\xi_{t+h}^\tau|\mathcal{F}_t] = {}^1\!/_2 E[\varepsilon_{t+h}\varepsilon_{t+h}^\tau|\mathcal{F}_t]$ for $h > 1$ (proof in Appendix B), and $\text{vec}(\Sigma_{t|t-1}) = (\Sigma_{t|t-1}^{1/2} \otimes \Sigma_{t|t-1}^{1/2})\,\text{vec}(I_K)$, we can obtain the VIRF of Hafner

and Herwartz (2006) with asymmetry:

$$
\begin{aligned}
V_1(\zeta_t, \mathcal{F}_{t-1}) &= E[\text{vech}(\Sigma_{t+1|t})|\mathcal{F}_{t-1}, \zeta_t] - E[\text{vech}(\Sigma_{t+1|t})|\mathcal{F}_{t-1}] \\
&= A^{\text{vech}}\Big[\,\text{vech}(\varepsilon_t\varepsilon_t^\tau) - \text{vech}(\Sigma_{t|t-1})\Big] - D^{\text{vech}}\Big[\,\text{vech}(\xi_t\xi_t^\tau) - 1/2\,\text{vech}(\Sigma_{t|t-1})\Big] \\
&= A^{\text{vech}}D_K^+\Big[\,\text{vec}(\varepsilon_t\varepsilon_t^\tau) - \text{vec}(\Sigma_{t|t-1})\Big] - D^{\text{vech}}D_K^+\Big[\,\text{vec}(\xi_t\xi_t^\tau) - 1/2\,\text{vec}(\Sigma_{t|t-1})\Big] \\
&= A^{\text{vech}}D_K^+(\Sigma_{t|t-1}^{1/2} \otimes \Sigma_{t|t-1}^{1/2})\,\text{vec}(\zeta_t\zeta_t^\tau - I_K) \\
&\quad - D^{\text{vech}}D_K^+\Big[\,\Big[\text{diag}\left\{\mathbb{1}_{x>0}(\Sigma_{t|t-1}^{1/2}\zeta_t)\right\}\Sigma_{t|t-1}^{1/2}\Big] \otimes \\
&\quad \Big[\text{diag}\left\{\mathbb{1}_{x>0}(\Sigma_{t|t-1}^{1/2}\zeta_t)\right\}\Sigma_{t|t-1}^{1/2}\Big]\,\Big]\,\text{vec}(\zeta_t\zeta_t^\tau - 1/2 I_K) \\
&= A^{\text{vech}}D_K^+(\Sigma_{t|t-1}^{1/2} \otimes \Sigma_{t|t-1}^{1/2})D_K\,\text{vech}(\zeta_t\zeta_t^\tau - I_K) \\
&\quad - D^{\text{vech}}D_K^+\Big[\,\Big[\text{diag}\left\{\mathbb{1}_{x>0}(\Sigma_{t|t-1}^{1/2}\zeta_t)\right\}\Sigma_{t|t-1}^{1/2}\Big] \otimes \\
&\quad \Big[\text{diag}\left\{\mathbb{1}_{x>0}(\Sigma_{t|t-1}^{1/2}\zeta_t)\right\}\Sigma_{t|t-1}^{1/2}\Big]\,\Big]D_K\,\text{vech}(\zeta_t\zeta_t^\tau - 1/2 I_K)
\end{aligned} \tag{30}
$$

$$
\begin{aligned}
V_2(\zeta_t, \mathcal{F}_{t-1}) &= E[\text{vech}(\Sigma_{t+2|t+1})|\mathcal{F}_{t-1}, \zeta_t] - E[\text{vech}(\Sigma_{t+2|t+1})|\mathcal{F}_{t-1}] \\
&= (A^{\text{vech}} + B^{\text{vech}} + 1/2 D^{\text{vech}})V_1(\zeta_t, \mathcal{F}_{t-1})
\end{aligned} \tag{31}
$$

$$
\begin{aligned}
V_h(\zeta_t, \mathcal{F}_{t-1}) &= E[\text{vech}(\Sigma_{t+h|t+h-1})|\mathcal{F}_{t-1}, \zeta_t] - E[\text{vech}(\Sigma_{t+h|t+h-1})|\mathcal{F}_{t-1}] \\
&= (A^{\text{vech}} + B^{\text{vech}} + 1/2 D^{\text{vech}})^{h-1}V_1(\zeta_t, \mathcal{F}_{t-1})
\end{aligned} \tag{32}
$$

E Conditional Volatility Profiles

To study the VIRF for an exogenous variable shock, we follow the method proposed by Gallant et al. (1993) and Lütkepohl (2005), the so-called conditional moment profiles, in which $g(\cdot)$ is a function of interest and δ expresses a shock hitting the system:

$$
E[g(\varepsilon_{t+h})|\delta, \mathcal{F}_t] - E[g(\varepsilon_{t+h})|\mathcal{F}_t] \tag{33}
$$

We then define the conditional volatility profiles by taking:

$$
g(\varepsilon_{t+h}) = [\varepsilon_{t+h} - E(\varepsilon_{t+h}|\mathcal{F}_{t+h-1})][\varepsilon_{t+h} - E(\varepsilon_{t+h}|\mathcal{F}_{t+h-1})]^\tau \tag{34}
$$

We now need to estimate and compare conditional covariance matrices with or without the shock to the system:

$$
\begin{aligned}
\widehat{\Sigma}_{t+h|t} &= E\{[\varepsilon_{t+h} - E(\varepsilon_{t+h}|\mathcal{F}_{t+h-1})][\varepsilon_{t+h} - E(\varepsilon_{t+h}|\mathcal{F}_{t+h-1})]^\tau|\mathcal{F}_t\} \\
\widehat{\Sigma}^{\delta}_{t+h|t} &= E\{[\varepsilon_{t+h} - E(\varepsilon_{t+h}|\mathcal{F}_{t+h-1})][\varepsilon_{t+h} - E(\varepsilon_{t+h}|\mathcal{F}_{t+h-1})]^\tau|\delta, \mathcal{F}_t\}
\end{aligned} \tag{35}
$$

Knowing that $E[\xi_{t+h}\xi_{t+h}^\tau|\mathcal{F}_t] = 1/2 E[\varepsilon_{t+h}\varepsilon_{t+h}^\tau|\mathcal{F}_t]$ for $h > 1$ (proof in Appendix B), we can write:

$$
\begin{cases}
\widehat{\Sigma}_{t+1|t} &= C^G_{t+1|t}C^{G\tau}_{t+1|t} + A^\tau E[\varepsilon_t\varepsilon_t^\tau|\mathcal{F}_t]A + B^\tau\Sigma_{t|t-1}B \\
&\quad + D^\tau E[\xi_t\xi_t^\tau|\mathcal{F}_t]D \\
\widehat{\Sigma}_{t+h|t} &= C^G_{t+h|t}C^{G\tau}_{t+h|t} + A^\tau E[\varepsilon_{t+h-1}\varepsilon_{t+h-1}^\tau|\mathcal{F}_t]A + B^\tau\widehat{\Sigma}_{t+h-1|t}B \\
&\quad + 1/2 D^\tau E[\varepsilon_{t+h-1}\varepsilon_{t+h-1}^\tau|\mathcal{F}_t]D \qquad \text{, for } h > 1
\end{cases} \tag{36}
$$

where C_t^G denotes the exogenous variable observed at time t. Moreover, we assume in this paper that $C_{t+h|t}^G = C_t^G$, as we do not model the exogenous variables and we do not have any forecasts available for these variables. Although assuming a VAR framework for the exogenous variable generation process would be possible, we kept the model as simple as possible to better track the impact of one-time shocks in the exogenous variables at time t.

Let us consider that $E[\varepsilon_t \varepsilon_t^\intercal | \mathcal{F}_t] = \widehat{\varepsilon}_t \widehat{\varepsilon}_t^\intercal$, where $\widehat{\varepsilon}_t$ corresponds to the residuals obtained through the VECM at time t. Likewise, we can write $E[\xi_t \xi_t^\intercal | \mathcal{F}_t] = \widehat{\xi}_t \widehat{\xi}_t^\intercal$ with $\widehat{\xi}_t = \widehat{\varepsilon}_t \circ \mathbb{1}_{x>0}(\widehat{\varepsilon}_t)$. Following Lütkepohl (2005), we consider $\Sigma_{t+h|t}$ to be a convenient estimator for $E[\varepsilon_{t+h} \varepsilon_{t+h}^\intercal | \mathcal{F}_t]$ with $h > 1$. We can then obtain the different conditional moment profiles for each given t and δ, $\Phi_{t,h}(\delta) = \widehat{\Sigma}_{t+h|t}^{\delta} - \widehat{\Sigma}_{t+h|t}$, and summarise all this information by averaging over t:

$$\Phi_{\cdot,h}(\delta) = \frac{1}{T-1} \sum_{t=2}^{T} \widehat{\Sigma}_{t+h|t}^{\delta} - \widehat{\Sigma}_{t+h|t} \tag{37}$$

F Volatility spillover

F.1 VMA representation

Following the definition of Diebold and Yilmaz (2009), we define the variance spillover effects as the measures of the proportion of system variance associated with asset interrelationships. To measure this, we have to decompose the forecast error variance associated with the VAR model. Diebold and Yilmaz (2012) augmented this concept of spillover by considering directional spillover. This latter enables us to track the proportion of variance that each asset transfers to the others, and symmetrically the proportion of variance that each asset receives from the others. Moreover, the authors improved this measurement by considering a generalised VAR framework (Koop et al., 1996; Pesaran & Shin, 1998), and thus they no longer rely on Cholesky's decomposition, which accordingly eliminates the dependence of the results on the variable ordering. However, provided that the measurement is based on a VAR model, they only generate static information. Diebold and Yilmaz (2012) used rolling windows to calculate a time-varying spillover index. Nevertheless, the spillover index thus obtained only represents the average value over the rolling sample. This is why Fengler and Herwartz (2018), building on the aforementioned works, proposed a dynamic spillover index based on a BEKK–MGARCH model. They used the forecast error variance decomposition of the vector moving average (VMA) representation associated with the squared and vectorised return process. Here, we propose to complement this approach by adding an asymmetric component and a set of exogenous variables to the BEKK–MGARCH model.

We first rewrite our BEKK–MGARCH model (equation (1)) in vech form. To this end, we use the elimination matrix L_K and the duplication matrix D_K, which, for a matrix X $(K \times K)$ are defined such that:

$$\begin{cases} \operatorname{vech}(X) & = L_K \operatorname{vec}(X) & \\ \operatorname{vec}(X) & = D_K \operatorname{vech}(X) & \\ D_K^+ & = L_K & \text{with } D_K^+ \text{ the Moore–Penrose inverse of } D_K \end{cases} \tag{38}$$

$$
\begin{aligned}
\Sigma_{t|t-1} &= C_t^G C_t^{G\tau} + A^\tau \varepsilon_{t-1}\varepsilon_{t-1}^\tau A + B^\tau \Sigma_{t-1|t-2} B + D^\tau \xi_{t-1}\xi_{t-1}^\tau D \\
\operatorname{vec}(\Sigma_{t|t-1}) &= \operatorname{vec}(C_t^G C_t^{G\tau}) + A^{\text{vec}} \operatorname{vec}(\varepsilon_{t-1}\varepsilon_{t-1}^\tau) \\
&\quad + B^{\text{vec}} \operatorname{vec}(\Sigma_{t-1|t-2}) + D^{\text{vec}} \operatorname{vec}(\xi_{t-1}\xi_{t-1}^\tau) \qquad \text{(see Appendix B)} \\
\operatorname{vech}(\Sigma_{t|t-1}) &= \operatorname{vech}(C_t^G C_t^{G\tau}) + D_K^+ A^{\text{vec}} D_K \operatorname{vech}(\varepsilon_{t-1}\varepsilon_{t-1}^\tau) \\
&\quad + D_K^+ B^{\text{vec}} D_K \operatorname{vech}(\Sigma_{t-1|t-2}) \\
&\quad + D_K^+ D^{\text{vec}} \left[\operatorname{diag}\left\{\mathbb{1}_{x>0}(\varepsilon_{t-1})\right\} \otimes \operatorname{diag}\left\{\mathbb{1}_{x>0}(\varepsilon_{t-1})\right\}\right] D_K \operatorname{vech}(\varepsilon_{t-1}\varepsilon_{t-1}^\tau) \\
&= C_t^{\text{vech}} + A^{\text{vech}} \operatorname{vech}(\varepsilon_{t-1}\varepsilon_{t-1}^\tau) \\
&\quad + B^{\text{vech}} \operatorname{vech}(\Sigma_{t-1|t-2}) + D_{t-1}^{\text{vech}} \operatorname{vech}(\varepsilon_{t-1}\varepsilon_{t-1}^\tau)
\end{aligned}
\tag{39}
$$

where diag denotes an operator that transforms a $K \times 1$ vector into a diagonal $(K \times K)$ square matrix, where the diagonal is the vector considered. Regarding the asymmetric component, the following identities:

$$
\begin{cases}
(\mathbf{A} \circ \mathbf{B})^\tau & = \mathbf{A}^\tau \circ \mathbf{B}^\tau \\
\operatorname{vec}(\mathbf{ABC}) & = (\mathbf{A} \otimes \mathbf{C}^\tau) \operatorname{vec}(\mathbf{B}) \\
\mathbf{a} \circ \mathbf{b} & = \operatorname{diag}(\mathbf{a})\mathbf{b} = \operatorname{diag}(\mathbf{b})\mathbf{a} \qquad \text{(Hadamard product of 2 vectors)}
\end{cases}
\tag{40}
$$

are used to obtain the equality:

$$
\begin{aligned}
\operatorname{vec}(\xi_{t-1}\xi_{t-1}^\tau) &= \operatorname{vec}\left\{\left[\varepsilon_{t-1} \circ \mathbb{1}_{x>0}(\varepsilon_{t-1})\right]\left[\varepsilon_{t-1} \circ \mathbb{1}_{x>0}(\varepsilon_{t-1})\right]^\tau\right\} \\
&= \operatorname{vec}\left[\operatorname{diag}\left\{\mathbb{1}_{x>0}(\varepsilon_{t-1})\right\} \varepsilon_{t-1}\varepsilon_{t-1}^\tau \operatorname{diag}\left\{\mathbb{1}_{x>0}(\varepsilon_{t-1})\right\}\right] \\
&= \left[\operatorname{diag}\left\{\mathbb{1}_{x>0}(\varepsilon_{t-1})\right\} \otimes \operatorname{diag}\left\{\mathbb{1}_{x>0}(\varepsilon_{t-1})\right\}\right] \operatorname{vec}(\varepsilon_{t-1}\varepsilon_{t-1}^\tau)
\end{aligned}
\tag{41}
$$

Then, following Fengler and Herwartz (2018), we note that $\eta_t = \operatorname{vech}(\varepsilon_t \varepsilon_t^\tau)$, and we consider $u_t = \eta_t - \operatorname{vech}(\Sigma_{t|t-1})$, which is a mean zero, serially uncorrelated, but conditionally heteroskedastic process, with $E[u_t u_t^\tau | \mathcal{F}_{t-1}] = \Omega_t$.

For the forthcoming demonstration, we also need to ensure that $\rho(\mathcal{A}_t) < 1$, where $\mathcal{A}_t = A^{\text{vech}} + B^{\text{vech}} + D_t^{\text{vech}}$ and $\rho(X)$ denotes the spectral radius of a square matrix X. We also define L as the lag operator, and $K^* = {}^{K(K+1)}/_2$. We can then express η_t as:

$$
\begin{aligned}
\eta_t &= C_t^{\text{vech}} + A^{\text{vech}} \eta_{t-1} + B^{\text{vech}}(\eta_{t-1} - u_{t-1}) + D_{t-1}^{\text{vech}} \eta_{t-1} + u_t \\
(I_{K^*} - \mathcal{A}_{t-1}L)\eta_t &= C_t^{\text{vech}} + (I_{K^*} - B^{\text{vech}} L) u_t \\
\eta_t &= (I_{K^*} - \mathcal{A}_{t-1}L)^{-1} C_t^{\text{vech}} + (I_{K^*} - \mathcal{A}_{t-1}L)^{-1}(I_{K^*} - B^{\text{vech}} L) u_t \\
&= \Phi_{t-1}(L) C_t^{\text{vech}} + \Phi_{t-1}(L)(I_{K^*} - B^{\text{vech}} L) u_t \\
&= \Phi_{t-1}(L) C_t^{\text{vech}} + \Theta_{t-1}(L) u_t
\end{aligned}
\tag{42}
$$

where $(I_{K^*} - \mathcal{A}_{t-1}L)^{-1}$ exists if and only if $\rho(\mathcal{A}_{t-1}) < 1$. We can then define $\Phi_t(L) = (I_{K^*} - \mathcal{A}_t L)^{-1} = \sum_{i \geq 0} \Phi_{t,i} L^i$, with $\Phi_{t,0} = I_{K^*}$ and $\Phi_{t,i} = \mathcal{A}_t \Phi_{t,i-1}, \forall i > 0$. In the same way, we can define $\Theta_{t,0} = I_{K^*}$, $\Theta_{t,1} = \mathcal{A}_t - B$, and $\Theta_{t,i} = \mathcal{A}_t \Theta_{t,i-1}, \forall i > 1$.

It is worth noting here that $E[u_t u_t^\tau | \mathcal{F}_{t-1}] = \Omega_t$ is not diagonal if the elements of u_t are simultaneously correlated, which thus impedes us from tracking the impact on the forecast error variance of a shock in u_t. To deal with this issue, Fengler and Herwartz (2018) proposed to rewrite the expression of η_t as follows:

$$
\eta_t = \Phi_{t-1}(L) C_t^{\text{vech}} + \Theta_{t-1}(L) \Omega_t^{1/2} \Omega_t^{-1/2} u_t \quad = \Phi_{t-1}(L) C_t^{\text{vech}} + \Psi_t(L) v_t \tag{43}
$$

where $v_t = \Omega_t^{-1/2} u_t$ and $\Psi_t(L) = \Theta_{t-1}(L)\Omega_t^{1/2}$, and so $\Psi_{t,i} = \Theta_{t-1,i}\Omega_{t-i}^{1/2}, \forall i \geq 0$.

We can therefore track for a given time t how unit shocks in the elements of v_t will simultaneously (for $i = 0$) and over time (for $i > 0$) impact the components of $\eta_t = \text{vech}(\varepsilon_{t-1}\varepsilon_{t-1}^\tau)$. We thus need to calculate $E[u_t u_t^\tau | \mathcal{F}_{t-1}] = \Omega_t$ to obtain $\Psi_{t,i}$ matrices. To do this, Fengler and Herwartz (2018) provide the following expression:

$$\Omega_t = L_K(\Sigma_{t|t-1}^{1/2} \otimes \Sigma_{t|t-1}^{1/2})\widetilde{\Omega}(\Sigma_{t|t-1}^{1/2} \otimes \Sigma_{t|t-1}^{1/2})L_K^\tau - \text{vech}(\Sigma_{t|t-1})\,\text{vech}(\Sigma_{t|t-1})^\tau \tag{44}$$

with $\widetilde{\Omega}$ a $K^2 \times K^2$ collecting the fourth-order moments (kurtosis) of $\zeta_t = \Sigma_{t|t-1}^{-1/2}\varepsilon_t$. Fengler and Herwartz (2018), based on the results of Lütkepohl (1997), demonstrated that this matrix is composed of $(K \times K)$ block matrices Ω_{ij}, with $\omega_{kl}^{(ij)}$ denoting the element on the k-th row and l-th column of the block matrix Ω_{ij} such that:

$$\begin{aligned} &\omega_{ii}^{(ii)} = \kappa_i, \qquad \omega_{jj}^{(ii)} = 1, \forall j \neq i, \qquad \omega_{ij}^{(ii)} = 0, \forall i \neq j \\ &\omega_{ij}^{(ij)} = 1, \qquad \omega_{kl}^{(ij)} = 0, \forall (k,l) \neq (i,j) \end{aligned} \tag{45}$$

As we assume a Gaussian distribution in this article, the kurtosis κ_i is equal to 3 for each asset.

F.2 Forecast error variance decomposition

We can then write the predicted error of η_{t+H}, with $\widehat{\eta}_{t+H|t} = E[\eta_{t+H}|\mathcal{F}_t]$, as:

$$\eta_{t+H} - \widehat{\eta}_{t+H|t} = \sum_{h=0}^{H-1} \Psi_{t+H,h} v_{t+H-h} \tag{46}$$

where the matrix $\Psi_{t+H,h}$ quantifies the impact of the innovation v_{t+H-h} on the H-step-ahead forecast error. The conditional forecast error variance then follows:

$$E[(\eta_{t+H} - \widehat{\eta}_{t+H|t})(\eta_{t+H} - \widehat{\eta}_{t+H|t})^\tau] = \sum_{h=0}^{H-1} \widehat{\Psi}_{t+H,h|t}\widehat{\Psi}_{t+H,h|t}^\tau \tag{47}$$

where $\widehat{\Psi}_{t+H,h|t} = \widehat{\Theta}_{t+H-1,h|t}\widehat{\Omega}_{t+H-h|t}^{1/2}, \forall h \in [\![0, H-1]\!]$.

Fengler and Herwartz (2018) proposed an approximation of the matrix $\widehat{\Omega}_{t+h|t} = \Omega_{t+h}(\Sigma_{t+h|t})$, so $\widehat{\Omega}_{t+h|t}$ will only depend on $\widehat{\Sigma}_{t+h|t}$, the forecast of the BEKK–MGARCH conditional covariance, and these are defined in equation (36):

$$\begin{cases} \widehat{\Sigma}_{t+1|t} &= C_{t+1|t}^G C_{t+1|t}^{G\tau} + A^\tau \widehat{\varepsilon}_t \widehat{\varepsilon}_t^\tau A + B^\tau \Sigma_{t|t-1} B + D^\tau \widehat{\xi}_t \widehat{\xi}_t^\tau D \\ \widehat{\Sigma}_{t+h|t} &= C_{t+h|t}^G C_{t+h|t}^{G\tau} + A^\tau \widehat{\Sigma}_{t+h-1|t} A + B^\tau \widehat{\Sigma}_{t+h-1|t} B \\ &\quad + 1/2 D^\tau \widehat{\Sigma}_{t+h-1|t} D \qquad \text{, for } h > 1 \end{cases} \tag{48}$$

We now need to express $\widehat{\Theta}_{t+H-1,h|t}$. Replacing $\Sigma_{t+1|t}$ in equation (39) with the expression of $\widehat{\Sigma}_{t+H|t}$ provided in equation (48), and η_t with the expression of $E[\eta_{t+H}|\mathcal{F}_t]$ provided in equation (42), one can note that we thus obtain two different expressions for $\widehat{\Theta}_{t+H-1,h|t}$. The first is for $H = 1$ and is the one-step-ahead forecast error variance decomposition, and the second is for $H > 1$.

For $H = 1$, the methodology and results are similar to those presented previously, that is: $D_t^{\text{vech}} = D_K^+ D^{\text{vec}} \left[\text{diag}\left\{\mathbb{1}_{x>0}(\varepsilon_t)\right\} \otimes \text{diag}\left\{\mathbb{1}_{x>0}(\varepsilon_t)\right\}\right] D_K$, $\mathcal{A}_t = A^{\text{vech}} + B^{\text{vech}} + D_t^{\text{vech}}$, and we need to ensure that $\rho(\mathcal{A}_t) < 1$.

However, for $H > 1$, the asymmetric component D_t^{vech} becomes $D^{\text{vech}} = {}^1\!/_2 D_K^+ D^{\text{vec}} D_K$, provided that $E[\xi_{t+H}\xi_{t+H}^\tau|\mathcal{F}_t] = {}^1\!/_2 E[\varepsilon_{t+H}\varepsilon_{t+H}^\tau|\mathcal{F}_t]$ (proof in Appendix B). As a consequence, the matrix D^{vech} no longer depends on t. Additionally, the condition $\rho(\mathcal{A}_t) < 1$ then becomes $\rho(\mathcal{A}) < 1$, in which $\mathcal{A} = A^{\text{vech}} + B^{\text{vech}} + D^{\text{vech}}$. Therefore, we have:

$$\begin{cases} \widehat{\Theta}_{t+H-1,0|t} = I_{K^*} & , \text{ for } H > 0 \\ \begin{cases} \widehat{\Theta}_{t,1|t} = \mathcal{A}_t - B^{\text{vech}} \\ \widehat{\Theta}_{t+H-1,1|t} = \mathcal{A} - B^{\text{vech}} \end{cases} & , \text{ for } H > 1 \\ \begin{cases} \widehat{\Theta}_{t,h|t} = \mathcal{A}_t \widehat{\Theta}_{t,h-1|t} & ,\forall h > 1 \\ \widehat{\Theta}_{t+H-1,h|t} = \mathcal{A}\widehat{\Theta}_{t+H-1,h-1|t} & ,\forall h > 1 \text{ and for } H > 1 \end{cases} \end{cases} \tag{49}$$

It is important to note that, in some instances, for a given t, the condition $\rho(\mathcal{A}_t) < 1$ may not be satisfied as the only constraint for the BEKK–GJR–MGARCH estimation is $\rho(\mathcal{A}) < 1$. In these particular cases, the one-step-ahead forecast error variance decomposition ($H = 1$) will not be available.

F.3 Construction of spillover indices

To estimate the different spillover indices proposed by Diebold and Yilmaz (2009), Diebold and Yilmaz (2012), or Fengler and Herwartz (2018) we define $\widehat{\psi}_{ij}^{(t+H,h|t)}$ as the element on the i-th row and j-th column of the matrix $\widehat{\Psi}_{t+H,h|t}$, and $\lambda_{t,ij}^{(H)}$ as the proportion of the H-step-ahead forecast error variance of variable i attributable to innovations in variable j:

$$\lambda_{t,ij}^{(H)} = \frac{\sum_{h=0}^{H-1} \left(\widehat{\psi}_{ij}^{(t+H,h|t)}\right)^2}{\sum_{h=0}^{H-1} \sum_{j=1}^{K^*} \left(\widehat{\psi}_{ij}^{(t+H,h|t)}\right)^2} \tag{50}$$

which means by construction that $\sum_{j=1}^{K^*} \lambda_{t,ij}^{(H)} = 1$, hence $\sum_{i,j=1}^{K^*} \lambda_{t,ij}^{(H)} = K^*$.

We then define the total variance spillover index $\mathcal{S}_t^H$, which represents the total proportion of the H-step-ahead forecast error variance resulting from spillover, such that:

$$\mathcal{S}_t^H = \sum_{i,j=1;i\neq j}^{K^*} \frac{\lambda_{t,ij}^{(H)}}{K^*} \tag{51}$$

The directional spillovers as defined by Diebold and Yilmaz (2012) are then denoted respectively $\mathcal{R}_{t,i}^H$, which represents the proportion of variance received by the variable i from the other variables, and $\mathcal{T}_{t,i}^H$ is the proportion of variance transmitted by the variable i to the other variables. It follows that the net contribution of each variable $\mathcal{N}_{t,i}^H$, which represents the difference between the volatility transmitted to the other variables and those received from them, can be expressed:

$$\mathcal{R}_{t,i}^H = \sum_{j=1;i\neq j}^{K^*} \frac{\lambda_{t,ij}^{(H)}}{K^*} \qquad \mathcal{T}_{t,i}^H = \sum_{j=1;i\neq j}^{K^*} \frac{\lambda_{t,ji}^{(H)}}{K^*} \qquad \mathcal{N}_{t,i}^H = \mathcal{T}_{t,i}^H - \mathcal{R}_{t,i}^H \tag{52}$$

As suggested by Fengler and Herwartz (2018), it is interesting to further distinguish spillovers between variances and covariances. To this end, we define $\mathcal{R}_{t,i}^{H,\text{cov}}$ as the directional spillovers received by the variable i from the covariances, while $\mathcal{T}_{t,i}^{H,\text{cov}}$ represents the directional spillovers

transmitted by the variable i to the covariances. Likewise, we define their net contributions $\mathcal{N}_{t,i}^{H,\text{cov}}$ and apply the same methodology to the variances:

$$\begin{aligned}
\mathcal{R}_{t,i}^{H,\text{cov}} &= \sum_{\substack{j\in I_{\text{cov}}\\ i\neq j}} \frac{\lambda_{t,ij}^{(H)}}{K^*} \qquad \mathcal{T}_{t,i}^{H,\text{cov}} = \sum_{\substack{j\in I_{\text{cov}}\\ i\neq j}} \frac{\lambda_{t,ji}^{(H)}}{K^*} \qquad \mathcal{N}_{t,i}^{H,\text{cov}} = \mathcal{T}_{t,i}^{H,\text{cov}} - \mathcal{R}_{t,i}^{H,\text{cov}} \\
\mathcal{R}_{t,i}^{H,\text{var}} &= \sum_{\substack{j\in I_{\text{var}}\\ i\neq j}} \frac{\lambda_{t,ij}^{(H)}}{K^*} \qquad \mathcal{T}_{t,i}^{H,\text{var}} = \sum_{\substack{j\in I_{\text{var}}\\ i\neq j}} \frac{\lambda_{t,ji}^{(H)}}{K^*} \qquad \mathcal{N}_{t,i}^{H,\text{var}} = \mathcal{T}_{t,i}^{H,\text{var}} - \mathcal{R}_{t,i}^{H,\text{var}}
\end{aligned} \tag{53}$$

Finally, we define specific spillover indices for covariances and variances (own or cross) as proposed by Fengler and Herwartz (2018), that is $\mathcal{S}_t^{H,\text{ocov}}$ ($\mathcal{S}_t^{H,\text{ovar}}$) and $\mathcal{S}_t^{H,\text{ccov}}$ ($\mathcal{S}_t^{H,\text{cvar}}$), which respectively represent the spillovers between all covariances (variances) and the spillovers from covariances to variances (from variances to covariances) such that:

$$\begin{aligned}
\mathcal{S}_t^{H,\text{ocov}} &= \sum_{i\in I_{\text{cov}}} \frac{\sum_{\substack{j\in I_{\text{cov}}\\ i\neq j}} \lambda_{t,ij}^{(H)}}{K^*} \qquad \mathcal{S}_t^{H,\text{ovar}} = \sum_{i\in I_{\text{var}}} \frac{\sum_{\substack{j\in I_{\text{var}}\\ i\neq j}} \lambda_{t,ij}^{(H)}}{K^*} \\
\mathcal{S}_t^{H,\text{ccov}} &= \sum_{i\in I_{\text{var}}} \frac{\sum_{\substack{j\in I_{\text{cov}}\\ i\neq j}} \lambda_{t,ij}^{(H)}}{K^*} \qquad \mathcal{S}_t^{H,\text{cvar}} = \sum_{i\in I_{\text{cov}}} \frac{\sum_{\substack{j\in I_{\text{var}}\\ i\neq j}} \lambda_{t,ij}^{(H)}}{K^*}
\end{aligned} \tag{54}$$

We note that, by construction, $\mathcal{S}_t^H = \mathcal{S}_t^{H,\text{ocov}} + \mathcal{S}_t^{H,\text{ovar}} + \mathcal{S}_t^{H,\text{ccov}} + \mathcal{S}_t^{H,\text{cvar}}$.

G Data

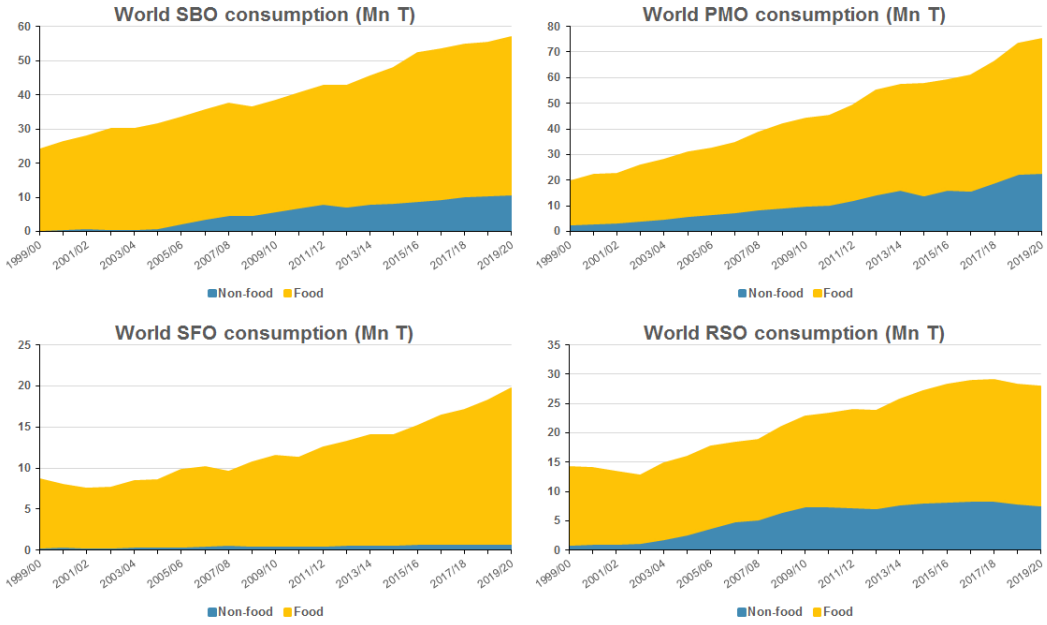

Figure G1: World vegetable oil consumption: food vs non-food uses.
Source: USDA-FAS (2020).

	2020	2019	2018	2017	2016	2015	2014
SBO	**10.70**	**11.27**	**10.82**	**9.80**	**9.21**	**9.18**	**8.06**
EU	0.87	0.91	0.71	0.68	0.69	0.43	0.49
USA	3.92	3.87	3.67	2.88	2.77	2.23	2.21
Argentina	1.60	2.15	2.43	2.87	2.66	1.81	2.58
Brazil	3.80	3.72	3.45	2.86	2.59	2.67	2.24
PMO	**16.85**	**17.62**	**14.74**	**11.65**	**10.81**	**8.60**	**10.21**
EU	4.16	4.49	4.24	4.22	3.60	3.33	3.28
USA	0.39	0.30	0.40	0.46	0.62	0.37	0.47
Colombia	0.55	0.58	0.57	0.54	0.51	0.51	0.52
Malaysia	0.80	1.20	1.09	0.72	0.50	0.67	0.60
Indonesia	7.70	7.48	5.37	2.97	3.18	1.22	2.92
Singapore	0.62	0.68	0.57	0.57	0.40	0.42	0.39
Thailand	1.37	1.55	1.32	1.15	1.07	1.10	1.04
RSO	**6.15**	**6.60**	**6.74**	**6.84**	**6.95**	**6.93**	**7.12**
EU	5.25	5.64	5.78	5.91	5.90	6.25	6.23
USA	0.53	0.56	0.54	0.66	0.51	0.34	0.47
SFO	**0.56**	**0.68**	**0.54**	**0.50**	**0.27**	**0.14**	**0.22**
EU	0.50	0.63	0.49	0.45	0.23	0.11	0.17
Used Cooking Oil	**4.34**	**5.12**	**4.44**	**3.97**	**3.66**	**3.03**	**2.65**
EU	2.30	2.80	2.64	2.33	2.05	1.85	0.65
USA	1.17	1.27	1.06	0.98	1.00	0.71	1.60
Biodiesel Output	**42.80**	**45.69**	**41.73**	**36.64**	**34.52**	**29.64**	**31.47**
EU	13.70	15.08	14.49	14.20	13.08	12.45	12.27
USA	7.30	7.35	7.20	6.15	6.25	4.77	4.80
Argentina	1.60	2.15	2.43	2.87	2.66	1.81	2.58
Brazil	5.20	5.16	4.68	3.75	3.33	3.46	3.00
Indonesia	7.70	7.48	5.37	2.97	3.18	1.22	2.92
EU Non-Biodiesel Uses							
RSO	4.05	4.30	4.22	4.11	4.26	4.33	3.96
SBO	1.70	1.70	1.53	1.48	1.49	1.45	1.52
PMO	3.68	4.02	3.89	3.54	3.89	3.76	3.84
SFO	4.96	4.47	4.36	4.12	3.72	3.61	3.65

Table G1: World biodiesel production and feedstocks used (million tonnes).
Note: EU Non-biodiesel uses are derived from the difference between each vegetable oil's domestic disappearance and its use for biodiesel production. *Source*: Oilworld (2020).

Figure G2: Major vegetable oil prices (daily, USD/T).
Source: Reuters (2021).

(a) Brent Price (USD/T)
Source: Reuters (2021).

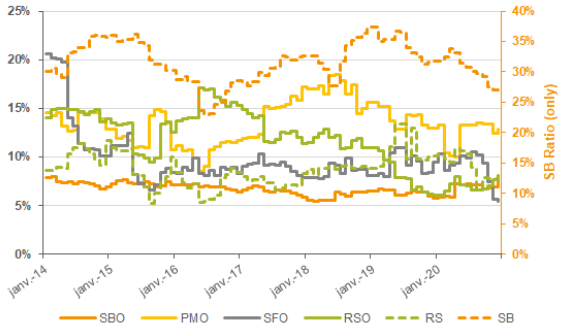

(b) Forecasted stock-to-use ratios.
Source: USDA (2021).

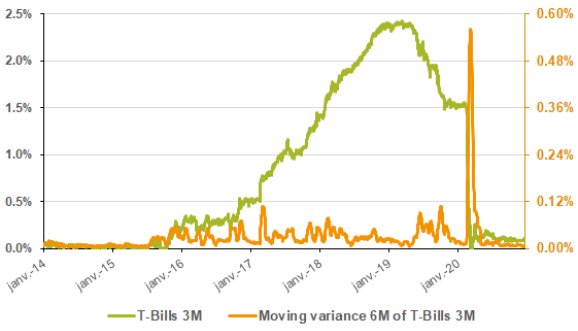

(c) Three-month Treasury bill rate.
Source: Federal Reserve (2021).

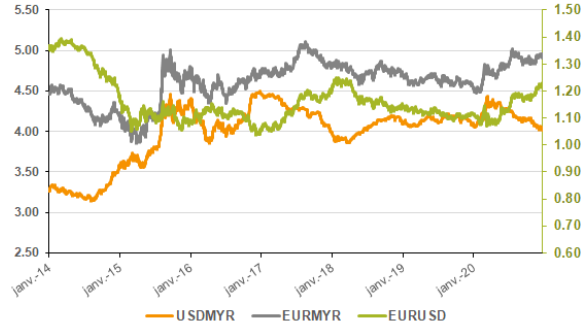

(d) Exchange rates.
Source: Reuters (2021).

Figure G3: Exogenous variables (daily).

H Volatility impulse response function

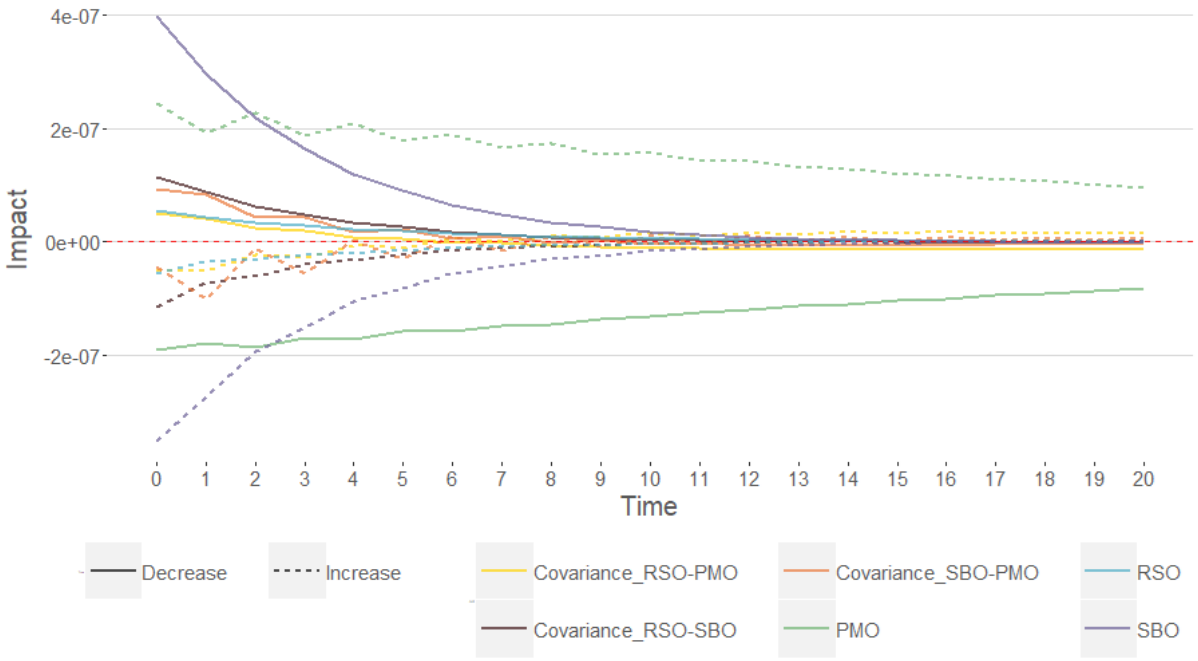

Figure H1: Volatility impulse response function (Brent price shock).